P1 1030139

THE UNITED STATES OF AMERICA

TO ALL TO WHOM THESE PRESENTS SHALL COME:

UNITED STATES DEPARTMENT OF COMMERCE
United States Patent and Trademark Office

June 26, 2003

THIS IS TO CERTIFY THAT ANNEXED HERETO IS A TRUE COPY FROM THE RECORDS OF THE UNITED STATES PATENT AND TRADEMARK OFFICE OF THOSE PAPERS OF THE BELOW IDENTIFIED PATENT APPLICATION THAT MET THE REQUIREMENTS TO BE GRANTED A FILING DATE.

APPLICATION NUMBER: *60/385,527*
FILING DATE: *June 04, 2002*
RELATED PCT APPLICATION NUMBER: *PCT/US03/17028*

By Authority of the
COMMISSIONER OF PATENTS AND TRADEMARKS

T. WALLACE
Certifying Officer

PRIORITY DOCUMENT
SUBMITTED OR TRANSMITTED IN COMPLIANCE WITH RULE 17.1(a) OR (b)

EXPRESS MAIL LABEL NO. EL726146346US

This is a Request for Filing a PROVISIONAL APPLICATION FOR PATENT under 37 CFR § 1.53(b)(2).

Docket Number→	UA.439P	Type a plus sign (+) inside this box →	+

INVENTOR(S)/APPLICATION(S)

Last Name:	First Name:	Middle Initial:	Residence (City and either State or Foreign Country):
Hartley Lorenzo	Tom Carl	T. F.	3649 Mogadore Rd., Mogadore, Ohio 44260 3275 W. 157th Street, Cleveland, Ohio 44111

TITLE OF THE INVENTION (280 characters max)

OPTIMAL BATTERY CHARGING FOR DAMAGE MITIGATION

CORRESPONDENCE ADDRESS:

Ray L. Weber
Renner, Kenner, Greive, Bobak, Taylor & Weber
First National Tower, Fourth Floor
Akron, Ohio 44308-1456
The United States of America

ENCLOSED APPLICATION PARTS (*check all that apply*)

X	Specification	Number of Pages	51	X	Small Entity Status
___	Drawing(s)	Number of Sheets	___	___	Other (specify) ^

METHOD OF PAYMENT OF FILING FEES FOR THIS PROVISIONAL APPLICATION FOR PATENT (*check one*)

X	A check or money order is enclosed to cover the filing fee	
___	The Commissioner is hereby authorized to charge filing fee and credit Deposit Account Number 18-0987	Filing Fee Amount(s): $80.00

The invention was made by an agency of the United States Government or under a contract with an agency of the United States Government:

X No.
___ Yes, the name of the U.S. Government agency and the Government contract number are: ^

Respectfully submitted,

Ray L. Weber, Reg. No. 26,519
Andrew B. Morton, Reg. No. 37,400
Renner, Kenner, Greive, Bobak, Taylor & Weber
First National Tower, Fourth Floor
Akron, Ohio 44308-1456
Telephone: (330) 376-1242

Date: June 4, 2002

___ Additional inventors are being named on separately numbered sheets attached hereto.

USE ONLY FOR FILING A PROVISIONAL APPLICATION FOR PATENT
SEND TO: Box Provisional Application, Assistant Commissioner for Patents, Washington, D.C. 20231

IN THE UNITED STATES PATENT AND TRADEMARK OFFICE

In the application of)
)
TOM T. HARTLEY and)
CARL F. LORENZO)
)
Serial No.)
)
Filed)
)
For OPTIMAL BATTERY)
CHARGING FOR DAMAGE)
MITIGATION)

Certificate of Mailing Via Express Mail

I hereby certify that this correspondence was deposited with the United States Postal Service as Express Mail - Label No. EL726146846US - "Express Mail Post Office to Addressee" service in an envelope addressed to: BOX PROVISIONAL APPLICATION, Assistant Commissioner of Patents and Trademarks, Washington, D.C. 20231 on this 4th day of June, 2002.

Debbie Tingler, Sec'y to Andrew B. Morton

TRANSMITTAL SHEET

Enclosed are the following documents:

Request for Provisional Application

Provisional Patent Application

Assertion of Small Entity Status *(w/Certificate of Mailing)*

Check in the Amount of $80.00

Return Receipt Postcard

The Commissioner is hereby authorized to charge payment of any fees associated with this communication or credit any overpayment to Deposit Account No. 18-0987. If a withdrawal is required from Deposit Account No. 18-0987, the undersigned attorney respectfully requests that the Commissioner of Patents and Trademarks cite Attorney Docket Number UA.439P for billing purposes.

Respectfully submitted,

Ray L. Weber, Reg. No. 26,519
Andrew B. Morton, Reg. No. 37,400
Renner, Kenner, Greive, Bobak,
Taylor & Weber
First National Tower, Fourth Floor
Akron, Ohio 44308-1456
Telephone: (330) 376-1242

Attorney Docket No: UA.439P

Optimal Battery Charging for Damage Mitigation

Tom T. Hartley
Professor of Electrical Engineering
The University of Akron
Akron, OH 44325-3904
TomHartley@aol.com

Carl F. Lorenzo
Distinguished Research Associate
NASA Glenn Research Center
Cleveland, OH 44135
Carl.F.Lorenzo@grc.nasa.gov

1.0 Introduction

This research proposes to use model-based control methods in the charging and discharging of batteries and fuel cells to provide improved performance and longer life.

Data from previous studies of NiH2 batteries is used to facilitate the research. Based on this data, a low order hybrid battery model is developed. This model contains some fractional order components due to the approximation of many diffusion processes in the battery. This model is then useable as a real-time observer. Damage mechanisms are studied for NiH2 batteries, which leads to the development of an instantaneous damage model. Using this knowledge, a control system is designed to extend battery life.

Fundamental to the success of this research is the development of an accurate and versatile dynamic model of the specific battery type. This is discussed in the next section. Damage modeling is then considered for the purpose of developing a control system that will extend battery lifetime. Advanced versions of a real-time observer and observer-based control, which include features such as model-parameter tracking, specific battery "learning," and damage mitigation, are discussed.

The experience gained with the NiH2 batteries should be extendable to Li based batteries and fuel cells. Similar procedures can be followed. It is expected that application of control methods to fuel cells should provide some immediate durability improvements, while the life of Li based batteries can be extended.

This research is highly interdisciplinary, as it combines the areas of electrochemistry, space power, control systems, dynamic modeling, fractional calculus, damage modeling, life-extending control, and power

electronics. An important consequence of this research is the ongoing information exchange between the various disciplines involved. Interdisciplinary research, such as this, which combines control systems and electrochemistry, is always fruitful, as it provides all parties with new and important insights into their fields of interest. It is believed that improved battery performance and extended lifetime can be obtained through operational improvements by the mechanism of optimal control design.

2.0 NiH2 Batteries

2.1 NiH2 Cells

Nickel-hydrogen cells have been used in space applications for many years. The main advantages of nickel-hydrogen cells are high specific energy, long cycle life, long functional lifetime, and fairly robust chemistry. The long cycle life has been used to advantage in low earth orbit (LEO) applications where a satellite will orbit the earth every 90 minutes. Roughly 35 minutes of this orbit is spent in the earth's shadow, during which time the satellite must use the batteries for power. The other 55 minutes of the cycle is spent in sunlight, during which time the satellite is powered by solar panels that must also recharge the batteries. In these applications, up to 50000 charge-discharge cycles are common for nickel-hydrogen cells. See Linden for more discussion of these cells.

Nickel-hydrogen cells are essentially a hybrid of standard cells and fuel cells. The **positive electrode** is nickel (NiOOH), and the **negative electrode** is hydrogen that diffuses into a porous platinum electrode. The platinum only serves to provide a reaction site for the hydrogen gas, and does not participate in the reaction. The entire cell consists of a large sealed pressure vessel that contains the hydrogen gas and the electrode stack. The electrode stack alternates pineapple-slice shaped disks of nickel electrode, **separator** (containing the electrolyte, KOH), platinum electrode, and a hydrogen diffusion **screen**. Collections of cells form a battery as shown in Figure 2.1.

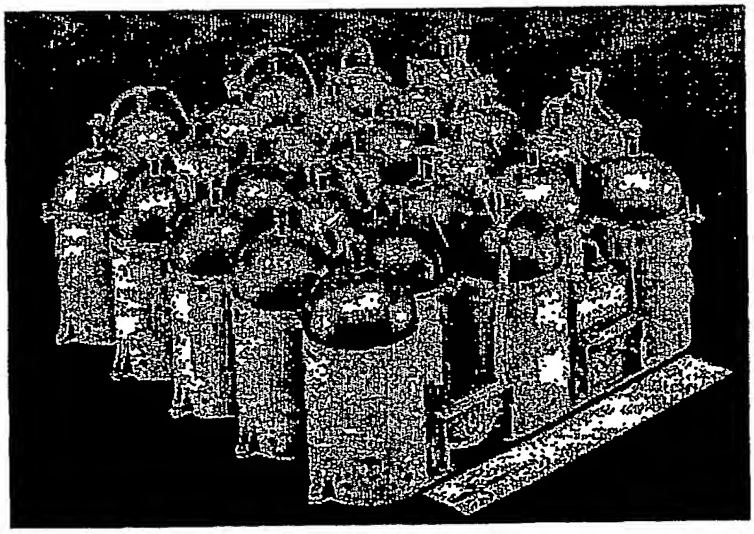

Figure 2.1 Typical NiH2 battery configuration (Briton & Miller).

2.2 NiH2 Cell Chemistry

In **normal charge-discharge operation** of a nickel-hydrogen cell, the electrochemical reactions are as follows:

positive nickel electrode: $$NiOOH + H_2O + e^- \underset{charge}{\overset{discharge}{\rightleftharpoons}} Ni(OH)_2 + OH^- \qquad (2.1)$$

negative hydrogen electrode: $$\tfrac{1}{2}H_2 + OH^- \underset{charge}{\overset{discharge}{\rightleftharpoons}} H_2O + e^- \ . \qquad (2.2)$$

During discharge at the positive electrode, the NiOOH (nickel oxy-hydroxide) on the electrode reacts with water in the electrolyte at the surface of the electrode as it accepts an electron from the external circuit through the nickel substrate. The products of this reaction are the $Ni(OH)_2$ (nickel hydroxide) on the electrode, and OH^- (hydroxyl ion) which diffuses away from the from the electrode through the electrolyte in the separator. At the negative electrode, the hydrogen gas reacts with hydroxyl ions in the electrolyte to form water and release an electron in to the external circuit. This process is reversed during charging. The electrolyte, which is often 31% KOH solution in water, contains potassium ions, K^+, and hydroxyl ions, OH^-, dissolved in water. Clearly the water and the hydroxyl ions are important in the reactions at the electrodes. It is usually assumed that the potassium ions do not take an active part in the cell reactions, however its exact role in the overall cell behavior is unclear.

During charging, **overcharge** reactions can occur. These occur whenever the charging current drives the above reactions faster than the required mass transfer can happen. This can occur both when the nickel electrode is fully charged, and when the charging current is too large. Thus, in overcharge, the nickel and the hydrogen do not participate in the reactions, and the electrolyte is reacting electrochemically at both electrodes. The overcharge reactions are as follows:

positive nickel electrode: $$2OH^- \xrightarrow{overcharge} H_2O + \tfrac{1}{2}O_2 + 2e^- \qquad (2.3)$$

negative hydrogen electrode: $$H_2O + \tfrac{1}{2}O_2 + 2e^- \xrightarrow{overcharge} 2OH^- \ . \qquad (2.4)$$

Consideration of these reactions would seem to indicate that overcharge is not a problem, but the formation of oxygen in a hydrogen environment is potentially very dangerous. This is discussed at greater length in the damage section below.

In a collection of cells composing battery, **cell reversal** can sometimes occur when a single cell discharges completely before other cells. This cell then becomes a load on the other cells. If the cell is assumed to be nickel limited, the reversal reactions are as follows:

positive nickel electrode: $$H_2O + e^- \xrightarrow{reversal} OH^- + \tfrac{1}{2}H_2 \qquad (2.5)$$

negative hydrogen electrode: $$\tfrac{1}{2}H_2 + OH^- \xrightarrow{reversal} H_2O + e^- \ . \qquad (2.6)$$

It should be observed that the hydrogen gas that is generated at the positive electrode is consumed at the same rate at the negative electrode. Thus there is no net increase in hydrogen pressure or any net change in

electrolyte concentrations during reversal, and the cell can be operated continuously in this mode. Cell reversal is not considered further in this paper.

3.0 Performance Model for NiH2 Batteries

3.1 Dynamic Modeling Background

Control systems are often used to improve the performance of many systems and devices (Friedland (1986)). Typically the quality of the control is related to the level of understanding of the system being controlled (Dorf (1974)). This system knowledge is contained the system dynamic model. Useful models for control design are dynamic, that is represented by differential equations, and are of reasonably low order (requiring only a few differential equations) while still capturing the important dynamics of the specific system (Hartley, Veillette, DeAbreu, Chicatelli, and Hartmann (1998)). A more complicated model, such as a computational fluid dynamic (CFD) model, will have thousands of differential equations (or dynamic states). This type of model is useful for a detailed understanding of battery phenomena and for cell design. Such a model, however, can contain states that are impractical to control, and can lead to a control system that is unnecessarily complex (Chicatelli and Hartley (1998)). Furthermore, a CFD model is often only represented as a computer code, and effectively no equations are available to the control system designer. On the other hand, a less complicated model, such as an empirical input-output relationship, may not contain any differential equations at all. This static model will usually not allow good control system design. Thus, to design a good control system, a low order dynamic model of the system to be controlled is most useful. This model should capture enough of the dynamic behavior of the system to be accurate over the frequency range of interest, while not being overly complicated.

In the area of battery and fuel cell modeling, there would appear to be two common types of model, CFD-based and empirical. The highly accurate CFD-based models are based on first principles, and accurately model the diffusion of all of the active species through whatever media are present (Doyle, Fuller, and Newman(1993), Newman(1991)). Such models require a large number of electrochemical parameters, including things such as ion mobilities and reaction rate constants. Also required is specific geometrical construction data on a given cell. These models are highly accurate and provide good representations of cell dynamics as long as the cell configuration remains constant. Unfortunately, as actual cells are charged and discharged, their dynamic parameters do not remain constant, and these models typically do not provide good representations for electrochemical cells over many charge-discharge cycles. Additionally, the exact construction varies from cell to cell, and thus these models do not quite have the actual cell information. In terms of using these models for control, there are also a large number of states due to the representation of many species diffusing through the cell. Furthermore, the spatial lumping of such diffusive systems usually yields a dynamic system that is very stiff (Hartley, Beale, and Chicatelli (1994)). Such systems are difficult to simulate, and rather than programming such a set of differential equations, an implicit simulation method is implemented directly on the diffusion equations in the computer code without the generation of any useful mathematical model on paper. Finally, these CFD-based models are expensive to build and change, while also being slow to build and use.

At the other modeling extreme from the CFD-based models are the empirical models. These model typically have a specific algebraic structure, and the model parameters are identified from given data (Shepherd(1965)). These are usually simple models that may provide reasonable static operating point representations of a given cell as it charges or discharges . Other than having a built in integral to track the charge, these models are usually not dynamic. Consequently, they can be considered as static maps, such as that of a transistor or of a compressor. Although they can predict an operating point, they do not accurately represent dynamic changes. Thus, the empirical models are not adequate for control system design.

A less common approach to battery and fuel cell modeling is what could be termed a hybrid model, or a performance model. Models of this type attempt to keep the important first principles dynamics, while not becoming so complicated as to not be readily useful. Their parameters are then tuned to match experimental data. This can be called essentializing the model. Such a model for electrochemical cells is discussed in Xia and Hartley (2000a, 2000b). This model has a chosen structure based on an electrochemical understanding of cell behavior. Given this dynamic model structure, the parameters of the model are determined for a given cell from charge-discharge data. An important aspect of this model is the representation of the many diffusion processes internal to the cell by a fractional order system (Lorenzo and Hartley(1998)). Consequently the model is of low order (few dynamic states with some fractional) and can be used for many different cell chemistries. A model of this type is fast, understandable, and amenable to control design. Furthermore, it is possible to update the parameters in the model as the cell changes through its charge-discharge cycles. Thus the hybrid modeling approach should provide a useful model structure for understanding cell changes through time, while also providing a useful dynamic model for control design.

3.2 Overview of NiH2 Cell Dynamics

As in most electrochemical systems, the dynamics of NiH2 cells are quite complex. This section presents an overview of the electrical and material behavior in a cell. Figure 3.1 gives a generic structure of the major components of the cell dynamics in normal operation. Here the electrical and material contributions have been separated for clarity. At each electrode, a voltage is generated between the electrode and the electrolyte based on the concentrations of reactants. The reactants then diffuse into the reaction site or away from the reaction site. The hydrogen gas must diffuse into the platinum electrode from the ambient chamber. The nickel compounds may not diffuse, but it is not clear if the reaction front at the nickel electrode is diffuse or not. Also, the hydroxyl ions and the water must diffuse from one electrode to the other through the electrolyte. The electrolyte diffusion represents a major resistance to the flow of charge through the cell. An additional source of electrical resistance is the charge transfer resistance at the electrode surface, across which there is also a double later capacitance. A voltage profile inside a typical cell is shown in Figure 3.2. There it is shown that voltage is produced between the electrode-electrolyte interfaces. It is shown later in this section that these voltages are dependent upon species concentrations on either side and on the current passing through. Additionally there is always an ohmic voltage loss in the electrolyte due to current passing through. It should be noted that this ohmic loss always corresponds to heating.

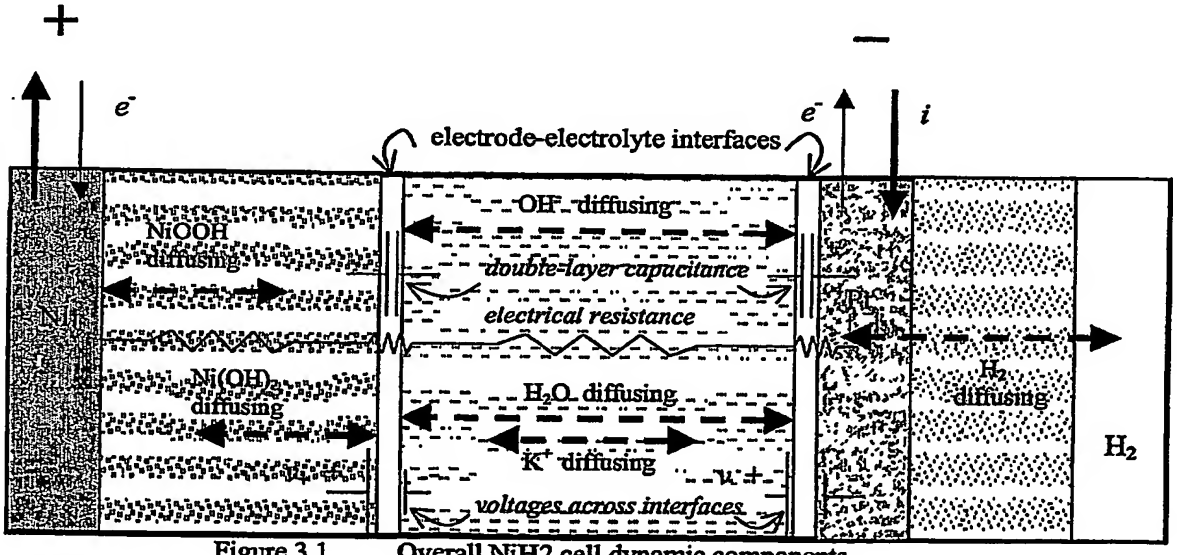

Figure 3.1 Overall NiH2 cell dynamic components.

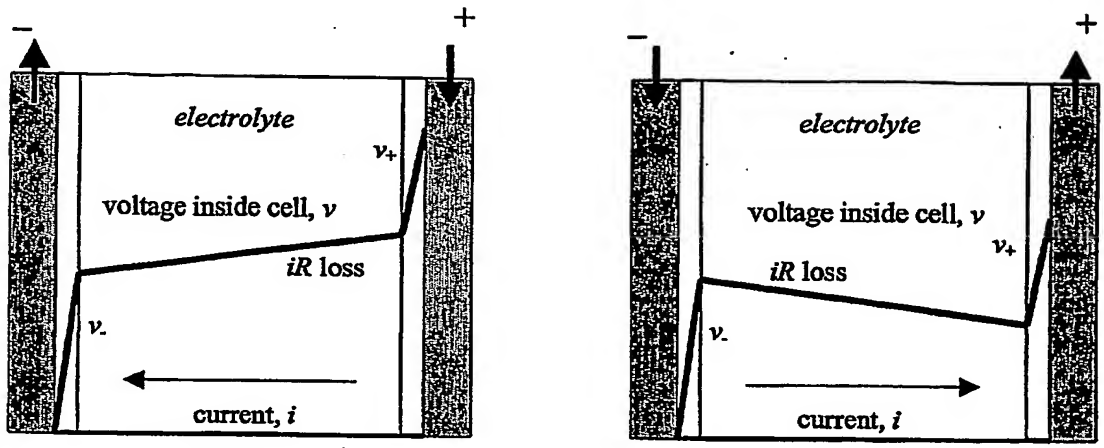

Figure 3.2 Typical voltage profiles inside a cell.

3.3 Model Essentialization

To extract the essence of the dynamics from the complex model given in Figure 3.1, several assumptions are made. The major assumption is that one electrode dominates the dynamics of the cell. In this case, we are assuming a hydrogen rich environment, and the nickel electrode is dominant in the dynamic behavior. At this electrode, we will only keep track of the amount of charged material, c_s, not the discharged material on the electrode. We will also lump all of the diffusive behavior into one fractional order term, c_d, which alleviates the need to model several diffusion channels in the cell. Finally, the voltage generated at the electrode will depend on the concentrations of both the stored material and the diffusing material at the electrode surface, and will be used as the terminal voltage. With these assumptions, the essential model is shown in Figure 3.3.

In the Figure 3.3, the electrical behavior is shown in the right side of the figure, and the chemical species behavior is shown on the left side. On the electrical side, the voltage at the terminals, v, is due to the dependent voltage source that is a function of electrical current, i, concentration of charged material, c_s, and concentration of diffusing material, c_d, at the electrode. On the chemical side, we are using an **electrical analogy of the material mass transfer.** In the analogy, mass flow rate becomes current (or flux), j, and material concentration becomes voltage. Thus the two dependent current sources on the chemical side are mass flow rates, j_s and j_d, defined by the current on electrical side. The charged material is stored in a capacitor, C, that represents mass storage, with the addition of the self-discharge resistor, R_{sd}, representing an orifice for the loss of charged material. The diffusing material must pass through a fractional-order element, ks^{-q}, that is an agglomeration of all the various diffusion pathways in the actual cell. This fractional-order element separates the concentration of diffusing material at the electrode, c_d, from the concentration in the bulk of the electrolyte, c_{bulk}.

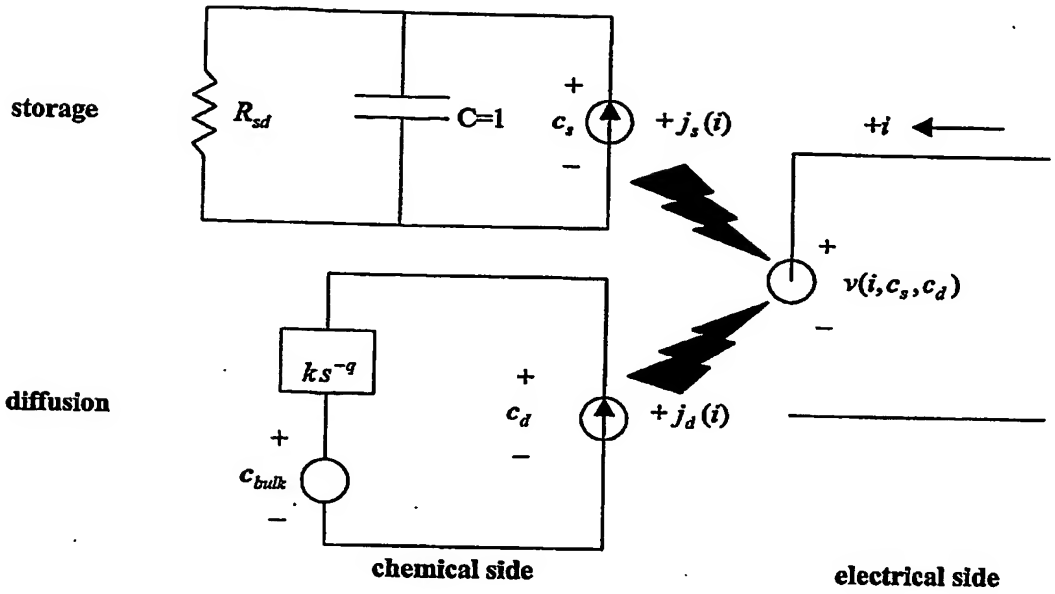

Figure 3.3 Essentialized performance model of NiH2 cell.

The effective chemical reaction in the cell then becomes

$$S + D + e^- \underset{\text{charge}}{\overset{\text{discharge}}{\rightleftharpoons}} \text{reaction products}, \qquad (3.1)$$

where charge conservation is assumed in the essentialized model. Here S represents the reacting stored material and D represents the reacting diffusing material. We will often associate the stored material in a NiH2 cell with NiOOH, and the diffusing material with either H_2O or OH^-, but this is only for mental imagery and not inherent to the math model We could also keep track of the reaction products if it were necessary for the accuracy of the model, but we have not needed to do that in our study. Based on this approximate cell reaction, during discharge, the stored material reacts with the diffusing material and an electron. Thus, when current is leaving the battery (electrons entering), both the stored and diffusing material are being deleted at the active electrode. Note that we could have assumed the diffusing material was building up outside the electrode during discharge, rather than going to zero, but that would have added a little more complexity.

The next several sections discuss the specifics of the various elements of the model. A discussion of the identification of the specific constants in the model is included. Note that a thermal model is not developed directly for the essentialized model. It is assumed that the heating effects are related to the cell damage, and that the damage model developed in Section 4.4 will contain the necessary information. Heating is considered further in Section 4.3 where energy flow, or power, in the cell is discussed.

3.4 Electrode Behavior: Faraday's Law

For the discussion of the next two sections, consider the electrode process :

$$aA+bB \longleftrightarrow cC+dD+ne^{-}. \tag{3.2}$$

This states that chemical species A and B are converted to species C and D plus electrons, at rates related to the coefficients a,b,c,d,n (it is also assumed that these compounds are appropriately ionized so that charge is conserved). It is important to understand that this equation represents both a chemical process and an electrical process. In fact, the reaction rates can be completely determined using the electrical process by recognizing that the chemical conversion can only occur if electrons are either arriving or leaving. Thus, the chemical conversion rates are controlled by, or measured by, the electrical current passing through a given electrode. All the rates of chemical conversion are then known via the following observation. For every n electrons leaving the electrode, c molecules of C are produced, d molecules of D are produced, a molecules of A are consumed, and b molecules of B are consumed. Then recognizing that the rate of electron production is related to electrical current i, the following rate equations result :

$$-i \equiv \frac{dq_{e^-}}{dt} = -\frac{d}{n}\frac{d\mathrm{D}}{dt} = -\frac{c}{n}\frac{d\mathrm{C}}{dt} = +\frac{a}{n}\frac{d\mathrm{A}}{dt} = +\frac{b}{n}\frac{d\mathrm{B}}{dt}, \tag{3.3}$$

Where q_{e^-} is the charge of a single electron. It should be noted that concentrations of chemical species are often used. Concentration is defined as moles of the species per unit volume. Concentrations are also often represented by [A] or by c_A, which would represent the concentration of species A. Using concentrations, the previous equation becomes

$$-i = nF\frac{dc_{e^-}}{dt} = -d\frac{dc_{\mathrm{D}}}{dt} = -c\frac{dc_{\mathrm{C}}}{dt} = +a\frac{dc_{\mathrm{A}}}{dt} = +b\frac{dc_{\mathrm{B}}}{dt} \tag{3.4}$$

where F is the Faraday constant relating the moles of electrons in a coulomb, F=96484.6 Coul/mole.

3.5 Electrode Behavior: Electrode Equation

Once the concentration rates on either side of the electrode interface are known, it is important to obtain an expression of the voltage in terms of these concentrations. This can be done by considering conservation of charge through the interface. Again assuming the reaction of Equation (3.2), the required relationship is determined by considering the fluxes, j, of the species in the forward and reverse reactions at the electrode,

$$i = j_f - j_r. \tag{3.5}$$

Assuming that the species fluxes are proportional to concentrations, yields

$$i = k_f c_A^a c_B^b - k_r c_C^c c_D^d. \tag{3.6}$$

Here, the rate constants, k, can be related to the electrical potential across the electrode-electrolyte interface using free energy considerations,

$$k_f = k_0 e^{(F/RT)(1-\alpha)(v-v_0)} \tag{3.7}$$

$$k_r = k_0 e^{(F/RT)(-\alpha)(v-v_0)} \tag{3.8}$$

where R is the universal gas constant, T is the temperature in K, α is an electrode energy barrier symmetry factor, $v - v_0$ is the voltage deviation from some nominal voltage v_0, and k_0 is a rate factor.

Inserting these gives the electrode equation,

$$i = k_0 \left(c_A^a c_B^b \, e^{(F/RT)(1-\alpha)(v-v_0)} - c_C^c c_D^d \, e^{(F/RT)(-\alpha)(v-v_0)} \right). \tag{3.9}$$

This equation is important to both the electrical and chemical behavior of the electrode-electrolyte interface as it relates the voltage across the interface to the concentrations of active species on either side of the interface and to the electrical current passing through the interface. It is often called the current-potential characteristic, and the approach used is often referred to as then Butler-Volmer approach (Bard and Faulkner (1980)).

Thus, for an electrode-electrolyte interface satisfying a reaction given by Equation (3.2), the required equations relating electrical current through the interface, electric potential across the interface, and species concentrations on either side of the interface are Equation (3.4) and Equation (3.9). These equations can also be used in a multiport configuration to relate and separate the electrical variables from the chemical variables. Consequently, these two equations are fundamental to representing the behavior of any electrified interface.

3.6 Linear-in-the-parameters Electrode Equation

The electrode equation is highly nonlinear, particularly when solving for the voltage in terms of the concentrations and the current. It is almost always solved using numerical methods, such as Newton – Raphson iteration. As an alternative to doing this, we propose a **linear-in-the-parameters approximate solution** to the electrode equation. The form we have chosen is

$$v = k_1 + k_2 \ln(1 + |i|)\mathrm{sgn}(i) + k_3 \ln(c_d) + k_4 \ln(1 - c_s) \tag{3.10}$$

where the variables i, c_s, c_d correspond to those in our essential model and the k's are parameters to be determined from data. What this equation assumes is that the terminal voltage v, is equal to the sum of four terms, and is effectively a compromise between the Tafel and the Nernst solutions of the electrode equation (Bard and Faulkner). The **Nernst solution** assumes that the current is so small as to be negligible. The electrode equation is then easily solved for the voltage in terms of the concentrations,

$$v = v_0 + \frac{RT}{nF} \ln\left(\frac{c_s}{c_d}\right). \tag{3.11}$$

Alternatively, the **Tafel solution** assumes that the current is large in one direction or the other, which means that one of the two exponential terms is negligible. With one of the exponentials equal to zero, the electrode equation is easily solved for the terminal voltage in terms of the current,

$$v = v_0 + \frac{RT}{\alpha nF} \ln(k_0) - \frac{RT}{\alpha nF} \ln(i). \tag{3.12}$$

In the linear-in-the-parameters approximate solution to the electrode equation, Equation (3.10), the first term is the constant k_1, which represents the voltage at the fully charged, zero current, steady state concentrations condition. It also represents the v_0 terms in the Nernst and Tafel solutions. The second term represents the nonlinear logarithmic dependence on current from the Tafel solution. The problem with the Tafel solution is that it assumes the current is large in one direction, but not both, while our approximation must be applicable to currents in both directions. Taking this into consideration yields our compromise term with the abs and sgn functions. The third and fourth terms represent the Nernst dependence on concentrations on either side of the charge storage reaction (and ignoring the fact that one reactant is in the solid state). The third term represents all the collective diffusion terms, as well as the electrolyte ions that are being consumed or generated at the electrode surface. As this concentration goes to zero, the terminal voltage gets small. As this concentration goes up, it has less and less effect on the voltage. The fourth and last term represents the effect of stored charge. As the stored charge approaches one, the voltage gets big. If it ever gets to zero, the voltage will also get small.

Another major benefit to our linear-in-the-parameters approximate solution is that it is possible to identify the 4 k-parameters directly from charge-discharge data using the batch or recursive least squares method (Goodwin and Sin). The requirement to do this is the actual measured terminal voltage and current, along with the estimated transient values of the stored charge and the diffusive material.

Note also that the **charge transfer resistance** through the double layer is contained implicitly in the current term in the linear-in-the-parameters approximation. Likewise, we are not modeling the **double-layer capacitance** explicitly, as it is also implicit in the linear-in-the-parameters approximation as well as the diffusive term.

3.7 Charge Storage

The charge storage will be through charge accumulation by integrating the current. Using the electrical analogy, this element is effectively capacitive. Any charge that passes into or out of the cell, will directly effect the concentration of the stored charge via Faraday's law,

$$\dot{c}_s(t) = i(t) \quad . \tag{3.13}$$

3.8 Diffusion Behavior

The diffusive components are lumped into one fractional-order term. This term effectively represents the diffusion of material toward or away from the electrode through the electrolyte, and with our assumed reaction, is thus on the same side of the reaction equation as the stored charge

$$S + D + e^- \underset{\text{charge}}{\overset{\text{discharge}}{\rightleftharpoons}} \text{reaction products.}$$

As a fractional-order element, its transfer function is

$$\frac{c_d(s)}{i(s)} = k_d s^{-q} \tag{3.14}$$

where s is the Laplace variable, and k_d and q are constant to be determined from data. However, the diffusive material concentration must return to the assumed bulk value when the system is quiescent. Thus the equation is converted to the time-domain and modified to reflect this return to bulk concentration

$$c_d(t) = c_{bulk} - k_d \, {}_0d_t^{-q} i(t). \tag{3.15}$$

It should be remembered that fractional-order terms have time-varying initialization functions associated with them. These were determined to have an overall effect on the diffusive terms of less than 3% our specific study, and were not included (ignored). If the implemented battery model is used in other ways after this study, the initialization functions may need to be included, which might also require further adjustment of the constants in Equation (3.15).

3.9 Self-discharge

Self-discharge is implemented through a simple resistive (to flow) loss across the charge storage element,

$$i_{sd} = \frac{c_s}{R_{sd}} \, . \tag{3.16}$$

This should be thought of as a pathway for stored material to leak out of storage (bigger R_{sd}, less loss).

3.10 Ohmic Cell Resistance

Most conducting media provide some resistance to the passage of electrical current. We could attempt to use one of the many ways that this is often calculated in electrochemical cells for our model, but we will allow the current term in the linear-in-the-parameters electrode equation to implicitly represent this resistance. If a value of resistance is needed, it can be obtained by linearizing the linear-in-the-parameters electrode equation. We will do that here since the resistance of a cell is often talked discussed. Noting that resistance can be defined from Ohm's law as

$$R \equiv \frac{dv}{di}, \tag{3.17}$$

then

$$R_{ohmic} = \frac{dv}{di} = \frac{d\left(k_1 + k_2 \ln(1+|i|)\mathrm{sgn}(i) + k_3 \ln(c_d) + k_4 \ln(1-c_s)\right)}{di}, \tag{3.18}$$

or

$$R_{ohmic} = \frac{dv}{di} = \frac{d\left(k_2 \ln(1+|i|)\mathrm{sgn}(i)\right)}{di}. \tag{3.19}$$

We can evaluate this for any steady-state current. Evaluating at zero steady-state current for symmetry gives

$$R_{ohmic} = \left[\frac{k_2}{1+|i_{ss}|}\right]_{i_{ss}=0} = k_2. \tag{3.20}$$

Thus the linear-in-the-parameters electrode equation gives a direct measure of the **total Ohmic resistance** in the cell at zero current, which includes both the charge transfer resistance at the electrodes, and the **Ohmic resistance** of the electrolyte.

3.11 Essentialized Model Overview

The model structure is given in Figure 3.3. The system dynamic equations are repeated below to highlight the required parameters.

Terminal behavior: **current into the battery is $+i$,** the terminal voltage is $+v$, (3.21)

stored material with self-discharge: $$\dot{c}_s(t) = i(t) - \frac{1}{R_{sd}} c_s(t), \quad (3.22)$$

diffusing material: $$c_d(t) = c_{bulk} - k_d \, {}_0d_t^{-q} i(t), \quad (3.23)$$

electrode equation: $$v(c_s, c_d, i) = k_1 + k_2 \ln(1 + |i|)\mathrm{sgn}(i) + k_3 \ln(c_d) + k_4 \ln(1 - c_s). \quad (3.24)$$

From this we can see that the required parameters are, self-discharge resistance R_{sd}, fractional-order q and constant k_d, bulk concentration of the diffusing material c_{bulk}, and the linear-in-the-parameters electrode equation constants, k_1, k_2, k_3, and k_4.

3.12 Parameter Determination

To most easily discuss the model parameter determination approach, we will apply it to a specific cell. The cell chosen is the NSWC Crane Pack ID 3602G (Gates). It is rated at 65 AHr, and uses 31% KOH concentration, and is maintained at 10 degrees C. The charge-discharge profile is a square wave, with 35% depth-of-discharge (DOD) and 104% recharge ratio. The square wave current is 26.29 A for 54 minutes charging, and –37.92 A for 36 minutes during discharge. Note that 65 AHr = 3900 AMin, 35% of 65 AHr = 1365.1 AMin = 26.29A*54Min, 3900AMin – 1365.1 AMin = 2534.9 AMin, and 104% of 1365.1 AMin =1419.7 AMin = 37.92A*36Min.

The self-discharge resistance is determined by the recharge ratio of 104%. We will assume that roughly half of the extra 4% goes into self-discharge, and that the other 2% goes into overcharge reactions. The division of the excess could be determined more accurately using the Buder method (Buder, 1972), but we have not done this at this time. Assuming no current in or out, we assume that 2% of the stored material (1.3 AHr = 78 AMin) is lost during each 90 Min cycle via self discharge. Using this in the known solution to Equation (3.22)

$$c_s(t) = c_s(0) e^{-t/R_{sd}} \quad (3.25)$$

gives

$$c_s(t) = 3900 - 78 = 3900 e^{-90/R_{sd}}. \quad (3.26)$$

Solving this for the self-discharge resistance gives $R_{sd}=4455$ ohms. This value was later modified after the simulation was implemented to force the constant-plus-taper charging to give a final charge of 3900AMin. The modified value of the self-discharge resistance that is used in the charging studies is $R_{sd}=4024$ ohms, or equivalently $1/R_{sd}=0.0002485$.

To determine q and k_d for the diffusive material, we will observe that most NiH2 cells are diffusion limited. This must be true, since the terminal voltages get small after only 35% of the active stored material is used. To start, it is assumed that the bulk concentration is unity,

$$c_{bulk}=1. \tag{3.27}$$

Thus we will assume that the diffusive material goes from unity concentration to roughly zero concentration as 35% of the stored material is used. With a constant current of –37.92 A, the solution to the diffusing material equation using Laplace transforms is

$$c_d(s)=\frac{1}{s}+\frac{k_d}{s^q}\frac{(-37.92)}{s}. \tag{3.28}$$

The time response obtained by inverse transforming this is

$$c_d(t)=1-37.92k_d t^q. \tag{3.29}$$

To determine the unknown constants, we will evaluate this at the end of discharge, or t=36 Min, at which point the concentration goes to roughly zero,

$$1-37.92k_d(36)^q=0,$$

or

$$37.92k_d(36)^q=1. \tag{3.30}$$

Taking the natural logarithm of both sides and rearranging gives

$$-\ln(37.92)=q\ln(36)+\ln(k_d). \tag{3.31}$$

This gives one equation for our two unknowns. If we now assume that the charging occurs similarly, we can obtain another equation. This is not exactly true, since the diffusive material will recover on its own, with no driving current, but this recovery is somewhat slower than the forced recovery. We will thus ignore the associated initialization response during the charging phase. Thus, charging at 26.29 A for 54 Min yields the equation

$$-\ln(26.29)=q\ln(54)+\ln(k_d). \tag{3.32}$$

These two equations can now be solved for the two unknowns, which become q=0.9034 and k_d=0.001036.

To implement the diffusion term, an approximation to the fractional operator is necessary. We will use the approximation of Sun, Abdelwahab, and Onaral (1984). The resulting approximation is

$$k_d s^{-0.9034}=0.001036\,\frac{0.0192s^2+1.1444s+0.3455}{s^2+0.5078s+0.0013} \tag{3.33}$$

which is designed with a maximum Bode magnitude response error of 2dB between $\omega = 10^{-3}$ and $\omega = 10^{+2}$. Better approximations containing more terms, or simpler approximations containing fewer terms are easily generated using the method. Again it should be noted that the initialization terms were ignored in this study.

The parameters in the electrode equation are obtained by using a batch least squares optimization on the charge-discharge data from the actual cell (see program in appendix). The resulting equation is

$$v = 1.3656 + 0.0265\ln(1+|i|)\mathrm{sgn}(i) + 0.0229\ln(c_d) - 0.0262\ln(1.005*3900 - c_s). \qquad (3.34)$$

Notice that the last term has been rescaled so that c_s can go to the AHr capacity of the battery, which is 3900AMin.

3.12 Model Verification Studies

Figures 3.4, 3.5, and 3.6 show actual charge-discharge data (the 'o' points) from the cell discussed in Section 3.12. These figures also contain the charge-discharge plot (solid line) from the identified model also discussed in Section 3.12. The three plots are chosen at 500 cycles, 10000 cycles, and 40000 cycles respectively to shown how the specific cell has changed with time, and to show the ability of the model to track changes in the cell.

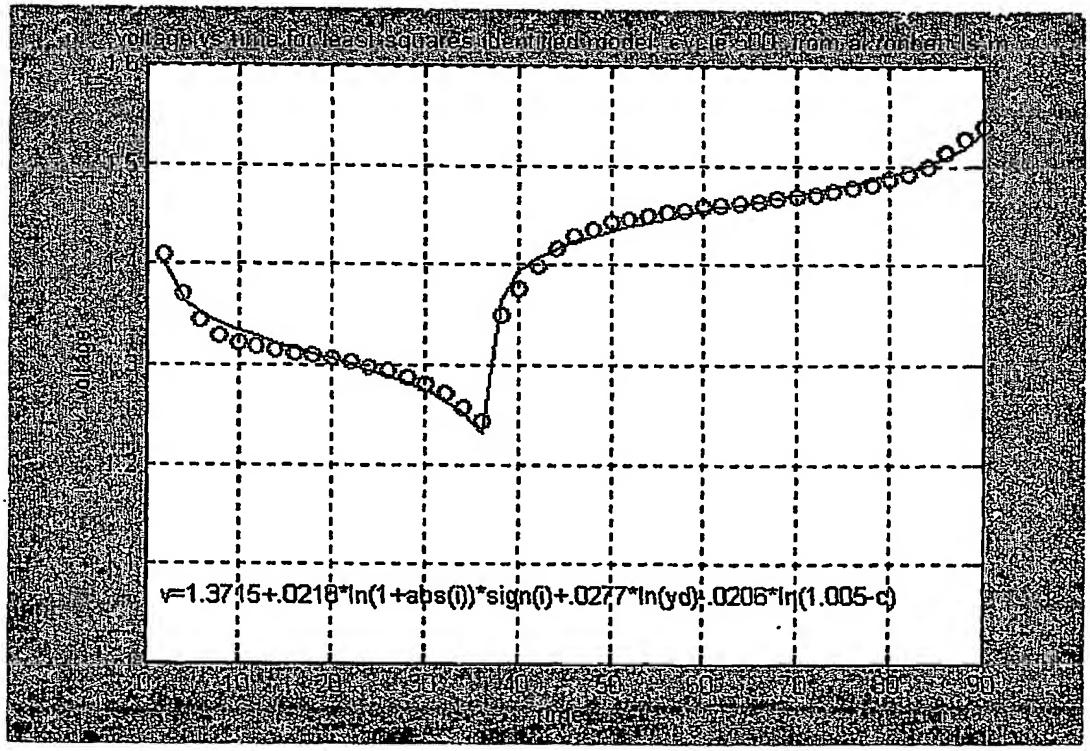

Figure 3.4. Charge-discharge cycle for the chosen cell at the 500th cycle.

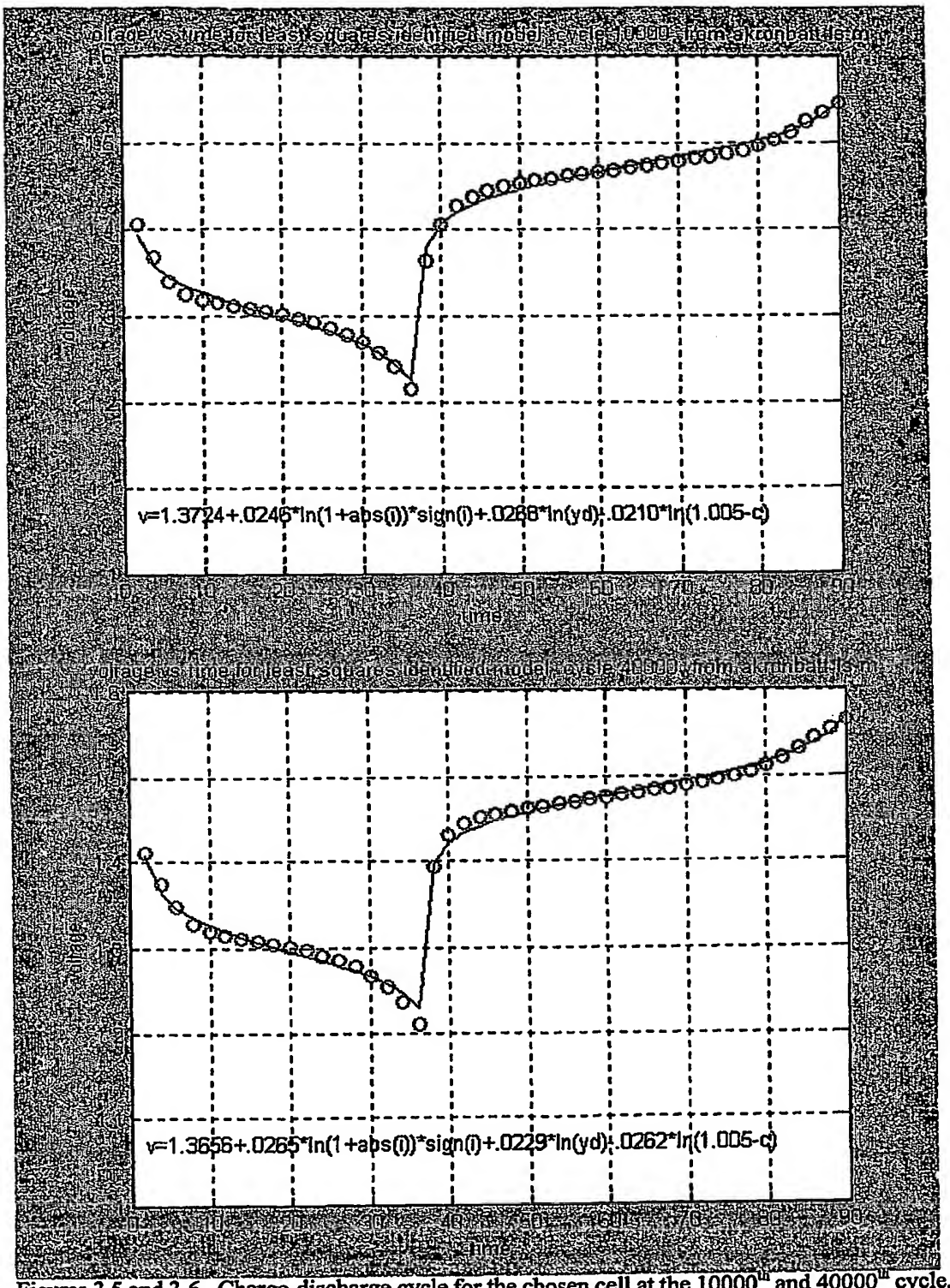

Figures 3.5 and 3.6. Charge-discharge cycle for the chosen cell at the 10000th and 40000th cycle.

4.0 Damage Modeling in NiH2 Batteries

4.1 Background

If the real-time observer is going to be able to provide information concerning the state of cell health, some understanding of the damage process in an electrochemical cell is necessary. There is no known instantaneous damage rate model for electrochemical systems, however, fatigue and creep damage modeling has been used for damage mitigating control in aerospace propulsion systems (Lorenzo (1994)). In that application, damage per cycle information has been used, as well as a continuum damage model developed. The continuum damage model predicts the current damage rate as a function of local stress and strain, and can be used to implement a controller that trades a small amount of performance (dynamic response) for large gains in system lifetime. A continuum damage model will be required for work with batteries and fuel cells.

For electrochemical cells and batteries, a number of damage mechanisms have been identified which include: corrosion, electrolyte communication between cells, separator dry out, popping damage, plaque expansion and electrochemical degradation. Still other mechanisms may be present which have not yet been identified. However it still remains to quantify these mechanisms, determine their importance to a particular design, and to determine the operational relationships to damage accumulation. These activities are beyond the scope of the current research, however as these effects are quantified, the resulting relationships can be used to refine battery damage prediction. The next two sections discuss in a general way the mechanisms that may be responsible for battery cyclic damage.

4.2 Damage Mechanisms for NiH2 Batteries

There are many ways to damage any cell. We will focus on the damage mechanisms that we think are presently the most significant for NiH2 cells.

Formation of γ - phase NiOOH:

At the positive nickel electrode, the charged material is NiOOH, and the discharged material is $Ni(OH)_2$. As in many solids, however, these compounds can exists in difference solid phases. The normal charge-discharge cycling occurs between the beta phases,

$$\beta\text{-NiOOH} \underset{\text{charge}}{\overset{\text{discharge}}{\rightleftharpoons}} \beta\text{-Ni(OH)}_2 \ .$$

On overcharge, however, the excess heating due to O_2 formation along with any large currents, causes the β-NiOOH to undergo a phase change into the γ-phase. γ-NiOOH possesses two properties of interest to our studies. One is that it generates a lower voltage with respect to the KOH electrolyte, roughly 1V and opposed to 1.5V for β-NiOOH. The other physical property is that the spaces between the molecules are much larger for γ-NiOOH than for β-NiOOH. Thus the formation of γ-NiOOH can physically damage a cell stack due to the changing size associated with the phase change. Additionally, as the amount of γ-NiOOH builds up, the usable charge storage capacity of the cell goes down, as the γ-NiOOH cannot provide the voltage necessary for the electrical loads.

Cells with a build-up of γ -NiOOH can be reconditioned using the reaction mechanism proposed by Bode. This is shown in Figure 4.1. It should be observed that the γ -NiOOH will cycle electrically with α -$Ni(OH)_2$. We can recover the original β -$Ni(OH)_2$ by allowing the cell to stand for an extended period of time in a KOH solution.

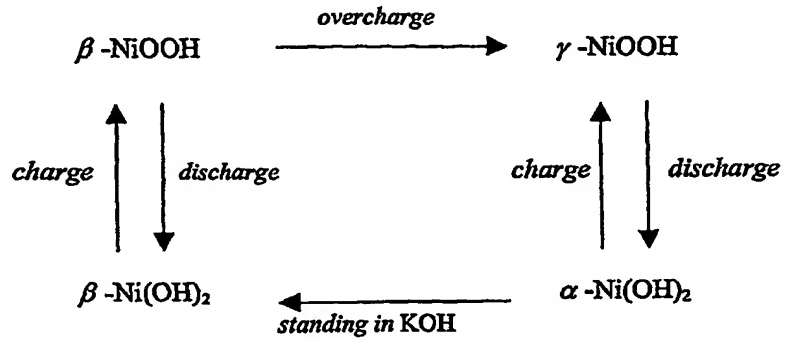

Figure 4.1 Solid phase relationships for a NiOOH electrode.

Formation of O2:

Overcharging a cell can occur by either continuing to charge the cell after all the β -$Ni(OH)_2$ has been converted to β -NiOOH, or when the charging current is so large that the β -$Ni(OH)_2$ cannot react fast enough to form β -NiOOH. In either case, the excess current goes into the electrolysis of the cell electrolyte. The effect of this is the formation of O_2 at the nickel electrode, along with heating. The problem is further complicated by the formation of oxygen in a hydrogen rich environment. These can recombine chemically and release significant heat. This recombination can also do physical damage to the electrode. This chemical recombination of oxygen and hydrogen is often called **popping**. Clearly, overcharging is to be avoided.

Heating:

Heating is a major problem in NiH2 batteries. As discussed above, it results in the formation of γ -NiOOH, which reduces cell capacity and does physical damage to the cell. Another problem with heating is the increase in self-discharge reaction rates, which can also be manifested as a reduction in cell capacity. Any excess heat production must be avoided.

4.3 Thermal Analysis and Hysteresis

This section will discuss the gross energy balances taking place in an electrochemical reaction. We will start with the free energy of the reaction,

$$\Delta G = \Delta H - T\Delta S. \tag{4.1}$$

Here ΔG is the Gibbs free energy of the reaction and represents the energy available for external work, and in electrochemical cells is effectively the source of the terminal voltage. ΔH is the enthalpy of the reaction and represents to total chemical energy change during the reaction. The $T\Delta S$ term is the temperature multiplied by the entropy change of the reaction. The entropy change involves the reordering of the reacting molecules as they undergo chemical reaction. Multiplying the entropy change by the temperature of the reactants, $T\Delta S$, gives the heat released or absorbed during the reaction. If the free energy is negative, the reaction will be spontaneous.

Dividing the above equation by $-nF$, where n is the number of electrons involved in the reaction and F is Faraday's constant, gives

$$-\frac{\Delta G}{nF} = -\frac{\Delta H}{nF} + \frac{T\Delta S}{nF}. \tag{4.2}$$

The sign convention of a spontaneous reaction giving a positive voltage in an electrochemical cell then gives

$$\Delta G = -nFv. \tag{4.3}$$

Using this in the energy equation yields

$$v = v_{TN} + \frac{T\Delta S}{nF}, \tag{4.4}$$

Here

$$\Delta H = -nFv_{TN} \tag{4.5}$$

is the thermoneutral voltage, or the voltage of the electrode reaction when there is no heat being generated. Although free energies, entropies, and enthalpies are all generally dependent on the concentrations of reactants, the enthalpy of reaction for many electrochemical reactions is roughly constant. This allows the thermoneutral voltage to be used as a measure of when there is heating at the reaction site by comparing it with the actual terminal voltage.

The energy flow in the reaction can be obtained by multiplying the above equation by the current,

$$iv = iv_{TN} + i\frac{T\Delta S}{nF}, \tag{4.6}$$

or

$$iv = iv_{TN} + Q_r. \tag{4.7}$$

Here Q_r is the rate of heat release or absorption at the reaction site, and represents the unavailable electrical power. This equation can be rearranged to give

$$Q_r = i(v - v_{TN}) \tag{4.8}$$

which shows that comparing the terminal voltage with the thermoneutral voltage allows determination of the heating due to the electrochemical reaction.

The above analysis has only considered the energy related to the electrochemical reaction, and has not considered any of the electrical behavior elsewhere in the overall cell, particularly any electrical losses. Whenever current flows in a conductor, there are electrical losses due to the heating of the material. We will use the total Ohmic resistance as the primary electrical heating source in this discussion. Doing so, we can write Equation (4.4) as

$$v = v_{TN} + \frac{T\Delta S}{nF} + iR_{Ohmic}. \tag{4.9}$$

This shows that the terminal voltage varies not only with the free energy of the reaction, but also with the resistive loss in the cell. Multiplying this equation by the current gives

$$iv = iv_{TN} + i\frac{T\Delta S}{nF} + i^2 R_{Ohmic}. \tag{4.10}$$

This equation can be expressed in words as:

electrical power = electrical power of the reaction + reaction heating/cooling + electrical heating.

Thus the overall heating is a combination of electrical and chemical effects.

The energy flow can be further generalized as in Sanabria, by including the energy that goes into oxygen production during overcharge. Equation (4.10) is generalized adding this electrolyzing current,

$$iv = (i-i_{O2})v_{TN} + (i-i_{O2})\frac{T\Delta S}{nF} + i_{O2}\left(v - iR_{Ohmic}\right) + i^2 R_{Ohmic}. \tag{4.11}$$

In words, this says:

electrical power in = electrical power into the reaction + reaction heating/cooling
+ heating due to O2 production + electrical heating.

The discussion of this section can be summarized in Figures 4.2 and 4.3 which show charge-discharge curves on a v-q diagram, along with the associated energy distribution as described by Equation (4.10). These diagrams are somewhat ideal in the sense that they do not have self-discharge or overcharge effects included. In the case of overcharge, the figure would need to be modified to reflect the current going to the oxygen production as described in Equation 4.11. Another important effect that is not considered in these figures, or the discussion above, is that the voltage can move up or down as the diffusing material relaxes (independent of the stored charge). Since only the stored charge is plotted on the horizontal axis, the figures do not take the concentration of diffusing material into effect.

At this point, sufficient data does not exist to quantify these effects for a particular battery design. Thus, based on available cycle life vs depth of discharge data we have developed an empirical continuum damage model for cells based on external variables, such as voltage and current, and internal variable such as species concentrations. It may be possible to explicitly include other internal variables, such as pressure and temperature in the future. This damage model allows the development of a damage mitigating control for NiH2 cells which is discussed in the next section.

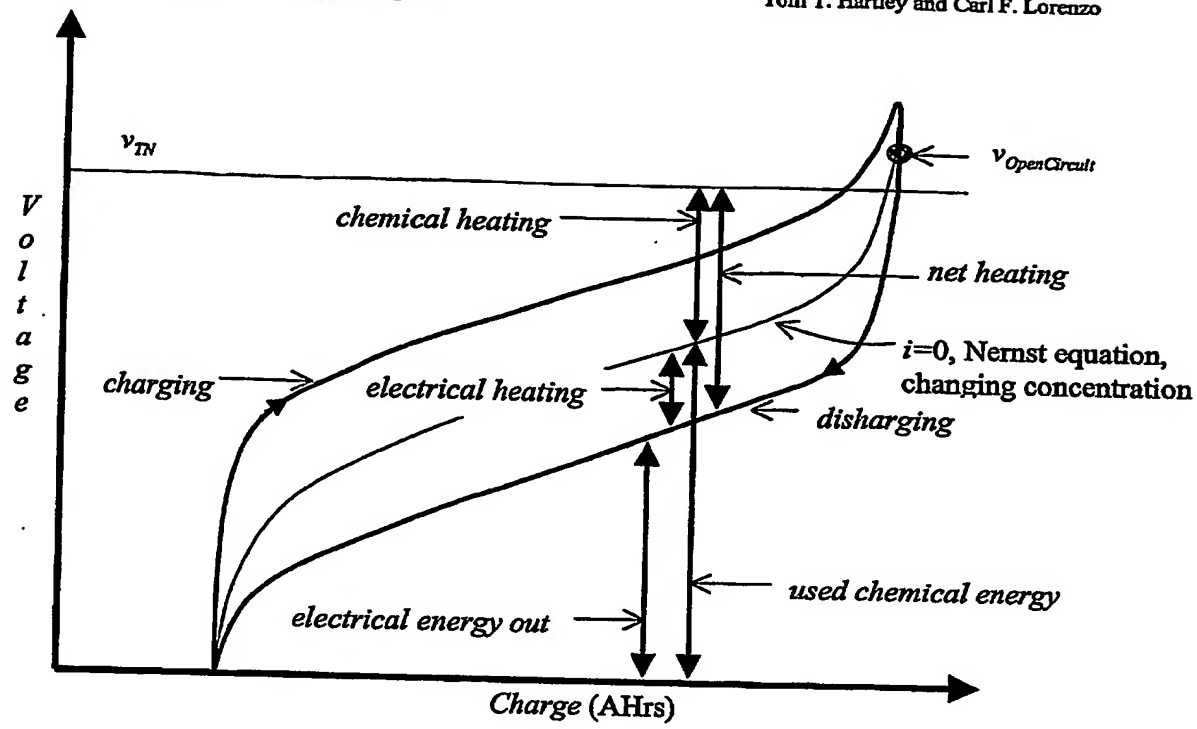

Figure 4.2 A typical charge-discharge cycle, showing the energy distribution during discharging.

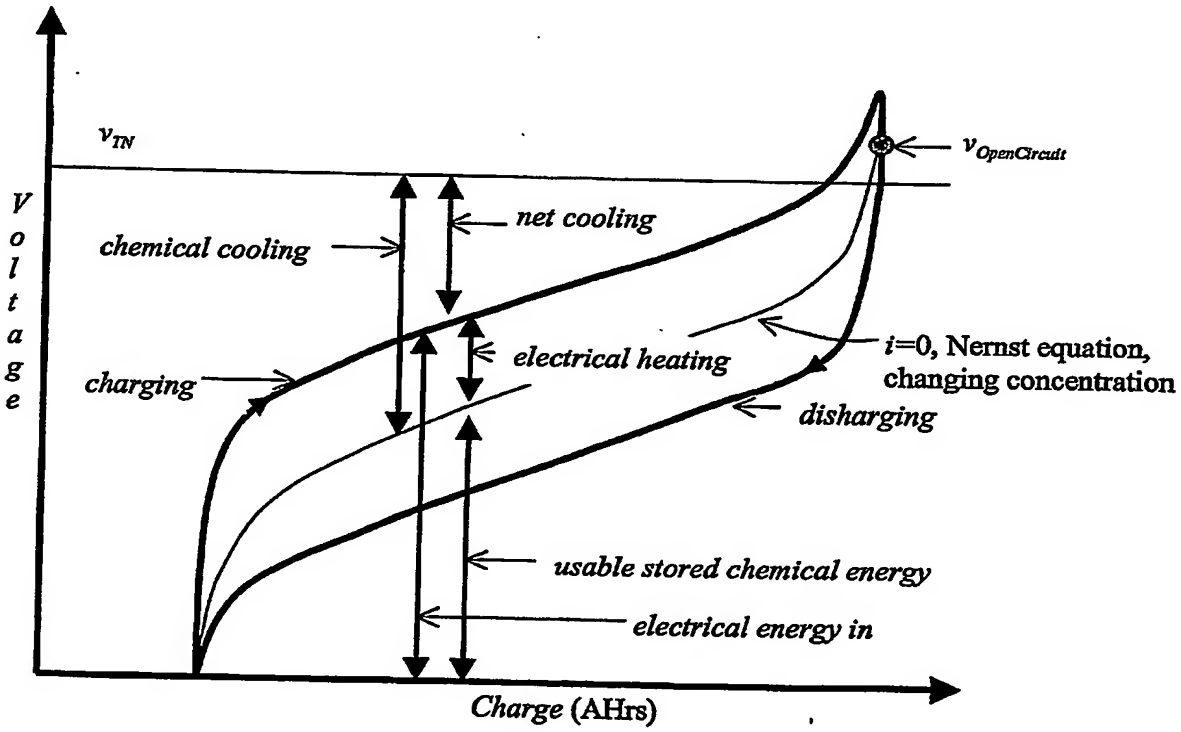

Figure 4.2 A typical charge-discharge cycle, showing the energy distribution during charging.

4.4 Battery Continuum Damage Modeling

This section develops methods for using battery cyclic life data to infer instantaneous damage rate within the battery. This instantaneous damage rate is required to design optimum charging profiles and to establish control algorithms. Cycle life as a function of depth of discharge (DOD) data for NiH2 cells is presented in the Green-Hoffman report. The following data from that report is given for a temperature of 10 degrees C,

DOD	Cycles To Failure
35%	38,000
50%	19,000

For this data, a charge/discharge cycle has a 90-minute period, with a 54 minute charging duration. The recharge ratio is always less than 110%, and the recharge current was constant until 94% recharge at which point a taper charge was used to finish the charging. The cycle life data is reproduced in Figure 4.3. In this figure, only two data points are available at 10 degrees C. Four curves have been fit to the data, the Green-Hoffman model, a modified Green-Hoffman model discussed later, a power law, and a linear curve. Although only the two Green-Hoffman approaches are considered, any curve can be fit through two points. The Green-Hoffman approach uses the following exponential model

$$N_{f\,GH} = 1885.04 e^{4.621(1-DOD)}, \qquad \text{at } 10^\circ \text{C} \tag{4.12}$$

where N_f is the number of cycles to failure. We will assume that when the total accumulated damage becomes equal to one, the cell has failed. Otherwise stated, the total accumulated damage is normalized to one. Further assuming that the damage per cycle is constant for a given DOD, or more specifically, that the damage per cycle does not increase as the accumulated damage increases, then the **damage per cycle** is

$$D_{cyc} = 0.0005305 e^{-4.621\,(1-DOD)} = \frac{1}{N_{f\,GH}}. \tag{4.13}$$

Based on similar previous studies of mechanical fatigue (Lorenzo), we will derive an expression for the **instantaneous damage**, $\dot{D}(t)$, based on the particular cycle life model. This is possible because the cycle life data implicitly contains all the information about how heating, overcharge, high current, and other hard to model factors damage a cell. The cyclic damage model expressed by equations (4.12) and (4.13) characterizes the damage hysteresis cycle size by DOD, which is actually representative of the charge amplitude of the cycle. The hysteresis cycle size could just as well be characterized by the voltage amplitude of the cycle. The purpose of the models to be derived here is to optimize the charging current profile. Models based on DOD as characterizing the size of the damage cycle are thus not useful because the overall charge to be stored during charging is always the same, no matter what charging profile is used. An alternative and more appropriate descriptor of cycle size for damage modeling is the voltage amplitude of the cycle. The voltage amplitude referenced to the minimum voltage point of the cycle (i.e. the discharge cutoff voltage

(35%)) will be used to describe the damage cycle. The stress variable then will be the voltage difference based on this reference voltage.

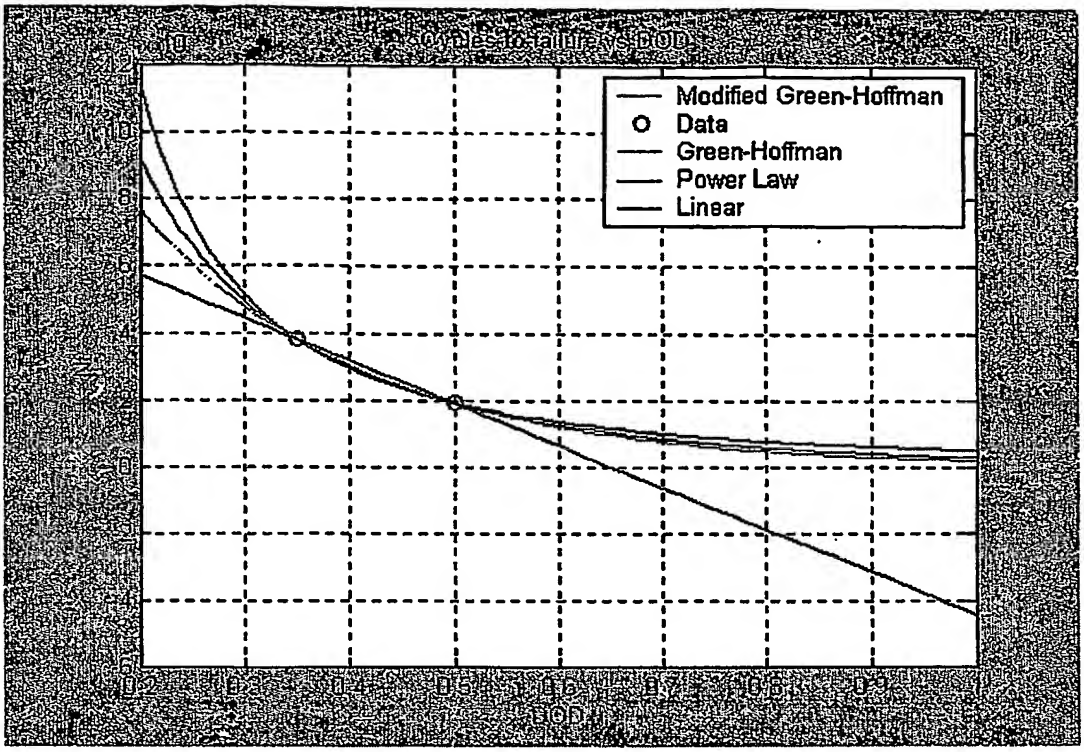

Figure 4.3 Cycle life vs DOD data.

For a full charge/discharge cycle, the voltage amplitude v_a varies with DOD (charge amplitude). This relationship is certainly a nonlinear function, but we will use a linear approximation. We express this as

$$DOD = c_1 v_a . \tag{4.14}$$

To obtain c_1, we adjust it until the simulated damage per cycle for a constant-plus-taper charge is equal to that given by Equation (4.13) for 35% DOD. This equation is substituted back into the damage per cycle, equation (4.13), giving

$$D_{cyc} = 0.0005305\, e^{-4.621+4.621 c_1 v_a} . \tag{4.15}$$

Now the accumulated damage as we traverse a charge/discharge cycle is the damage per cycle. Thus the integration of the instantaneous damage through the cycle is

$$\int_{cycle}\hat{\delta}(v)\,dv = D_{cyc} = 0.0005305\,e^{-4.621+4.621c_1v_a}. \tag{4.16}$$

where $\hat{\delta}(v)$ is the **voltage referred damage rate**, that is

$$\hat{\delta}(v) = \frac{dD}{dv}. \tag{4.17}$$

We now assume that all of the damage is accumulated over the charging part of the cycle, that is the "uphill" part of the process, then

$$\int_{v_{min}}^{v_{max}}\hat{\delta}(v)\,dv = D_{cyc} = 0.0005305\,e^{-4.621+4.621c_1v_a} = 5.222\times10^{-6}e^{4.621c_1v_a}. \tag{4.18}$$

We note that models including damage on the discharging portion of the cycle are readily possible using techniques similar to those used here. Changing the limits of integration gives

$$\int_{0}^{v_{max}-v_{min}}\hat{\delta}(v+v_{min})\,dv = 0.0005305\,e^{-4.621+4.621c_1v_a} = 5.222\times10^{-6}e^{4.621c_1v_a}. \tag{4.19}$$

Since $v_a = v_{max} - v_{min}$, we can now infer an approximation to the shifted voltage referred damage rate, $\hat{\delta}(v+v_{min})$, as

$$\hat{\delta}(v+v_{min}) \cong 0.0005305e^{-4.621}4.621c_1e^{4.621c_1v} \tag{4.20}$$

The reason that this is approximate is due to the fact that at cyclic amplitude of $DOD = v_a = 0$, the Green-Hoffman model does not yield zero cyclic-damage, as we require. In fact, as discussed in Section 4.2, zero amplitude would actually allow healing. Then Equation (4.20) becomes

$$\hat{\delta}(v) = 2.4129\times10^{-5}c_1e^{4.621c_1(v-v_{min})}. \tag{4.21}$$

This result in Equation (4.18) gives

$$\int_{v_{min}}^{v_{max}}\hat{\delta}(v)\,dv = 5.222\times10^{-6}\left(e^{4.621c_1v_a}-1\right) \cong 5.222\times10^{-6}\,e^{4.621c_1v_a}. \tag{4.22}$$

Once the voltage referred damage rate is obtained, the **instantaneous damage rate** can be obtained by simple application of the chain rule

$$\dot{D}(t) \equiv \frac{dD}{dt} = \frac{dD}{dv}\frac{dv}{dt} = \hat{\delta}(v(t))\,\dot{v}(t). \tag{4.23}$$

We require of our model that damage, $D(t)$, be a monotonically increasing function, that is, the model will be conservative in that, healing of the battery will not be not allowed. Therefore we require the instantaneous damage rate to always be positive, thus equation (4.23) is modified to

$$\dot{D}(t) \equiv \frac{dD}{dt} = \frac{dD}{dv}\left|\frac{dv}{dt}\right| = \hat{\delta}(v(t))\,|\dot{v}(t)|. \tag{4.24}$$

Substituting the voltage referred damage rate into this equation gives the instantaneous damage rate as

$$\dot{D}(t) = 5.222\times10^{-6} c_1\, e^{4.621 c_1 (v - v_{\min})}\,|\dot{v}(t)|. \tag{4.25}$$

Choosing v_{min}=1.2V, gives at last

$$\dot{D}(t) = 5.222\times10^{-6} c_1\, e^{4.621 c_1 (v - 1.2)}\,|\dot{v}(t)|. \tag{4.26}$$

This is the continuum damage model based on the Green-Hoffman cyclic damage model.

Modified Damage Model

The Green-Hoffman exponential model, equations (4.12) and (4.13), implies that cyclic damage occurs when the depth of discharge is zero. This is not physically plausible for an operational battery damage model. The degradation that occurs during shelf storage is not the same as cyclic damage. Thus we will modify the Green-Hoffman model so that cyclic damage goes to zero as depth of discharge goes to zero. For the model to allow zero damage at zero DOD we require the cyclic damage to have the form

$$D_{cyc} = c_2\left(e^{c_3 DOD} - e^{c_3 0}\right) = c_2\left(e^{c_3 DOD} - 1\right) = \frac{1}{N_f} \tag{4.27}$$

The constants c_2 and c_3 are determined numerically to best fit the data presented in the table at the beginning of this section. This process yields the damage per cycle as

$$D_{cyc} = 1.0404\times10^{-5}\left(e^{3.602 DOD} - 1\right) = \frac{1}{N_f}. \tag{4.28}$$

For DOD =35%, then this equation gives $D_{cyc} = 2.6316\text{x}10^{-5}$. To get the instantaneous damage, we will again assume a linear relationship between DOD (the charge amplitude) and cyclic amplitude of voltage deviation,

$$DOD = c_1 v_a. \tag{4.29}$$

To obtain c_1, we adjust it until the simulated damage per cycle for a constant-plus-taper charge is equal to that given by Equation (4.28) for 35% DOD. Finding c_1 must wait until the end of the process however. This equation can be substituted back into the damage per cycle

$$D_{cyc} = 1.0404\times10^{-5}\left(e^{3.602 c_1 v_a} - 1\right) \tag{4.30}$$

Then, the integral of voltage referred damage rate, $\hat{\delta}(v)$, for one charging cycle must be equal to the damage per cycle, and assuming damage formation only during the during the charging phase of the cycle

$$\int_{v_{min}}^{v_{max}} \hat{\delta}(v)\,dv = D_{cyc} = 1.0404\times10^{-5}\left(e^{3.602 c_1 v_a} - 1\right). \tag{4.31}$$

where

$$\hat{\delta}(v) = \frac{dD}{dv} \tag{4.32}$$

is the voltage referred damage rate and $D(t)$ is the accumulated damage. Changing the limits of integration of Equation (4.31) gives

$$\int_{0}^{v_{max}-v_{min}} \hat{\delta}(v+v_{min})\,dv = \int_{0}^{v_a} \hat{\delta}(v+v_{min})\,dv = 1.0404\times10^{-5}\left(e^{3.602 c_1 v_a} - 1\right). \tag{4.33}$$

The shifted voltage referred damage rate $\hat{\delta}(v+v_{min})$ is now determined to be

$$\hat{\delta}(v+v_{min}) = 1.0404\times10^{-5}\,(3.602 c_1) e^{3.602 c_1 v} \tag{4.34}$$

or

$$\hat{\delta}(v) = 3.7475\times10^{-4}\, c_1\, e^{3.602 c_1 (v-v_{min})}, \qquad v > v_{min}. \tag{4.35}$$

This voltage referred damage rate exactly satisfies Equation (4.31). Having the voltage referred damage rate, the instantaneous damage rate can again be obtained by application of the chain rule

$$\dot{D}(t) \equiv \frac{dD}{dt} = \frac{dD}{dv}\frac{dv}{dt} = \hat{\delta}(v(t))\dot{v}(t). \tag{4.36}$$

Further requiring that the instantaneous damage rate is always positive gives

$$\dot{D}(t) \equiv \frac{dD}{dt} = \frac{dD}{dv}\left|\frac{dv}{dt}\right| = \hat{\delta}(v(t))\,|\dot{v}(t)|. \tag{4.37}$$

Substituting the incremental damage rate into this equation gives the instantaneous damage rate as

$$\dot{D}(t) \equiv 3.7475\times10^{-4}\, c_1\, e^{3.602 c_1 (v-v_{min})}\,|\dot{v}(t)|. \tag{4.38}$$

Choosing v_{min}=1.2V, gives

$$\dot{D}(t) \equiv 3.7475\times10^{-4}\, c_1\, e^{3.602 c_1 (v-1.2)}\,|\dot{v}(t)|. \tag{4.39}$$

Now, adjusting c_1 until the simulated damage per cycle for a constant-plus-taper charge is equal to that given by Equation (4.28) for 35% DOD, that is $D_{cyc} = 2.6316\text{x}10^{-5}$, yields $c_1 = 0.9707$.

It should be noted that the instantaneous damage rate could also be expressed as a function of the current and rate of change of voltage with charge by continued application of the chain rule,

$$\dot{D}(t) \equiv \frac{dD}{dt} = \frac{dD}{dv}\left|\frac{dv}{dq}\right|\left|\frac{dq}{dt}\right| = \hat{\delta}(v(t))\left|\frac{dv}{dq}\right|\,|i(t)|. \tag{4.40}$$

Here dv/dq is the slope of the charging curve on the v-q diagram.

In deriving Equation (4.37), we required that the instantaneous damage rate always be positive. This was accomplished by using the absolute value of the voltage rate. This is justifiable in that whenever the voltage rate becomes large positive or negative, there are significant microscale changes taking place in the cell. An alternative result would be to have the damage rate go to zero whenever the voltage rate goes negative. This is justifiable in that the cell may not be undergoing damage when it is relaxing, that is, when the voltage rate is negative. Clearly, this topic requires further study. The damage rate in this case becomes

$$\begin{aligned} \dot{D}(t) &= 3.7475\times10^{-4}\, c_1\, e^{3.602 c_1 (v-1.2)}\, \dot{v}(t), \quad \dot{v}(t) \geq 0 \\ \dot{D}(t) &= 0, \qquad\qquad\qquad\qquad\quad \dot{v}(t) < 0 \end{aligned} \tag{4.41}$$

In this case, the constant $c_1 = 1.0901$.

From the various forms for the damage, Equations (4.36)-(4.41), it can be seen that changing voltage is indicative of damage in the cell. The rate of change of voltage is an indication that the chemical reactions are proceeding in a manner to cause damage on a microscopic level. Thus keeping the voltage from changing abruptly should allow longer life in these cells. This would seem to indicate that a "soft take-off" and a "soft landing" are important in the charging process to avoid damaging the cell. Looking back at the energy balance equations with or without O2 production, Equations (4.10) or (4.11) give the following expression for the voltage rate

$$\dot{v}(t) = \frac{1}{nF}\frac{d(T(t)\Delta S(t))}{dt} + R_{Ohmic}\frac{di(t)}{dt}. \tag{4.42}$$

In words this equation says:

changing terminal voltage $\propto$ changing heat of reaction + changing heating due to current,

that is, the heating rate is intrinsically tied to the damage process. Stated differently, or on a microscopic scale, the equation indicates

changing terminal voltage $\propto$ changing microscopic reordering rate + changing material flow rate.

This is because the current is proportional to the concentration as indicated by equations (3.3) and (3.4). Both of these processes involve the rate of change of material, that is, material motion and acceleration, which would be related to internal damage rate. This would seem to infer that damage rate and internal loss rates are related, thus justifying the use of voltage-difference rate as the continuum damage rate model stress variable.

Now that we have an instantaneous damage rate model, we can use it to design an optimal charging profile that minimizes the accumulated damage per cycle. This will be the topic of Section 5.

4.6 Effect of Damage in the Essentialized Model

This section will discuss the incorporation of the accumulated damage into the dynamic performance model. First it is important to associate the accumulated damage with some physical mechanism. We will associate the accumulated damage with the inability to store charge, or to accumulate the stored material. Thus this could be associated with the formation of the γ - phase NiOOH, which actually does reduce the possible total stored charge. Likewise, overcharging always causes heating, which leads to the formation of γ - phase NiOOH. Consequently, we will associate the accumulated damage with a reduction in the ability to accumulate the stored material.

The inability to store charge could potentially be manifested into all of the parts of the performance model; Faraday's Law, the electrode equation (or the linear-in-the-parameters form), the charge storage term, the diffusion term, or the self-discharge. As we are associating the damage with a reduction in the inability to accumulate the stored material, we will focus on incorporating the damage into the charge storage term. Equation (3.22) becomes

stored material with self-discharge and damage:
$$\dot{c}_s(t) = i(t) - \frac{1}{R_{sd}} c_s(t) - \dot{D}(t). \qquad (4.43)$$

But, as we have used the linear-in-the-parameters electrode equation, it must also be modified to indicate a loss of capacity. Thus Equation (3.24) becomes

electrode equation with damage:
$$v = k_1 + k_2 \ln\left(1 + |i|\right)\mathrm{sgn}(i) + k_3 \ln(c_d) + k_4 \ln\left(\left(1 - D(t)\right) - c_s\right). \qquad (4.44)$$

5.0 Damage Mitigating Control

5.1 Control Philosophy

Control system design is usually separated into at least two phases. Phase one is the design of optimal trajectories and associated inputs, that move a given plant from one operating condition to another, while minimizing some performance measure. This subject is the topic of the present section and the next. Phase two is the design of a trajectory following controller (sometimes called a regulator or tracker) that provides a real-time control input perturbation to keep the plant operating near the designed optimal trajectory. This is discussed in Section 7.

Our **control philosophy** is to charge the NiH2 cell in such a way that the damage incurred during the charging period is minimized, thus extending its cycle life. This is generally considered **damage mitigating control** or **life-extending control**. We will call the optimal charging profile **life-extending charge**. A damage mitigating control for use during discharge could also be considered, but the required discharge current was dependent on time-varying mission needs, and would require hardware modifications that were considered outside the scope of this research. Some discussion of possible damage mitigating strategies for discharge is included in the discussion of Section 8.

5.2 Performance Measure

The performance measure to be minimized is the accumulated damage per recharge cycle. This can be obtained by integrating instantaneous damage rate with respect to time:

$$J = \int_0^{t_f} \dot{D}(t)\,dt, \tag{5.1}$$

where $\dot{D}(t)$ is obtained from either of the damage models, Equations (4.26) or (4.39), and t_f for our problem is 54 Min. As it is, this performance measure can be minimized by using zero current, which does not recharge the cell. Thus, the performance measure must contain some information on the total charge required during charging. This is easily incorporated into a final state weighting term:

$$J = w_{fs}\left(c_s^*(t_f) - c_s(t_f)\right)^2 + \int_0^{t_f} \dot{D}(t)\,dt, \tag{5.2}$$

where $c_s^*(t_f)$ is the desired stored charge at the end of charge (≤ 1), w_{fs} is the cost weighting associated with the error in stored charge at the end of charge, and again $\dot{D}(t)$ is obtained from either of the damage models, Equations (4.26), (4.39), or (4.41), and t_f for our problem is 54 Min. Note that only one weighting term is necessary as it can be either greater or less than unity, but is constrained to be positive. In the implementation, we have chosen the self-discharge resistance to have a value which forces the final charge using constant-plus-taper charge (104% of 1420AMin) to have a value of 3900AMin. The optimizer forces the life-extending charge to also have this final value. The constant charge (also 104% of 1420AMin) will have a final charge larger than this since the self-discharge current is slightly less than the constant-plus-taper.

5.3 Original Optimization Approach

To determine the optimal charging profile, or life-extending charge, that minimizes the performance measure, Equation 5.2, we will use a numerical optimization approach. The algorithm used is outlined in Figure 5.1. Some typical charging results are shown in Figures 5.2 a-d.

```
Load previous best
Set j=1
    Guess u(jT)
      Initialize simulation
                Main simulation loop
                        Derivative function evaluations
                        Numerical integration (Euler, T=1)
                        Damage rate calculation
                        Integrate damage rate
                End main loop
                Include final state error into Performance Measure
            Change u(jT) using gradient search and repeat until optimal
    Increment j and repeat
Reset j=1 and repeat until optimal
Store present best
```

Figure 5.1. Outline of original optimization approach.

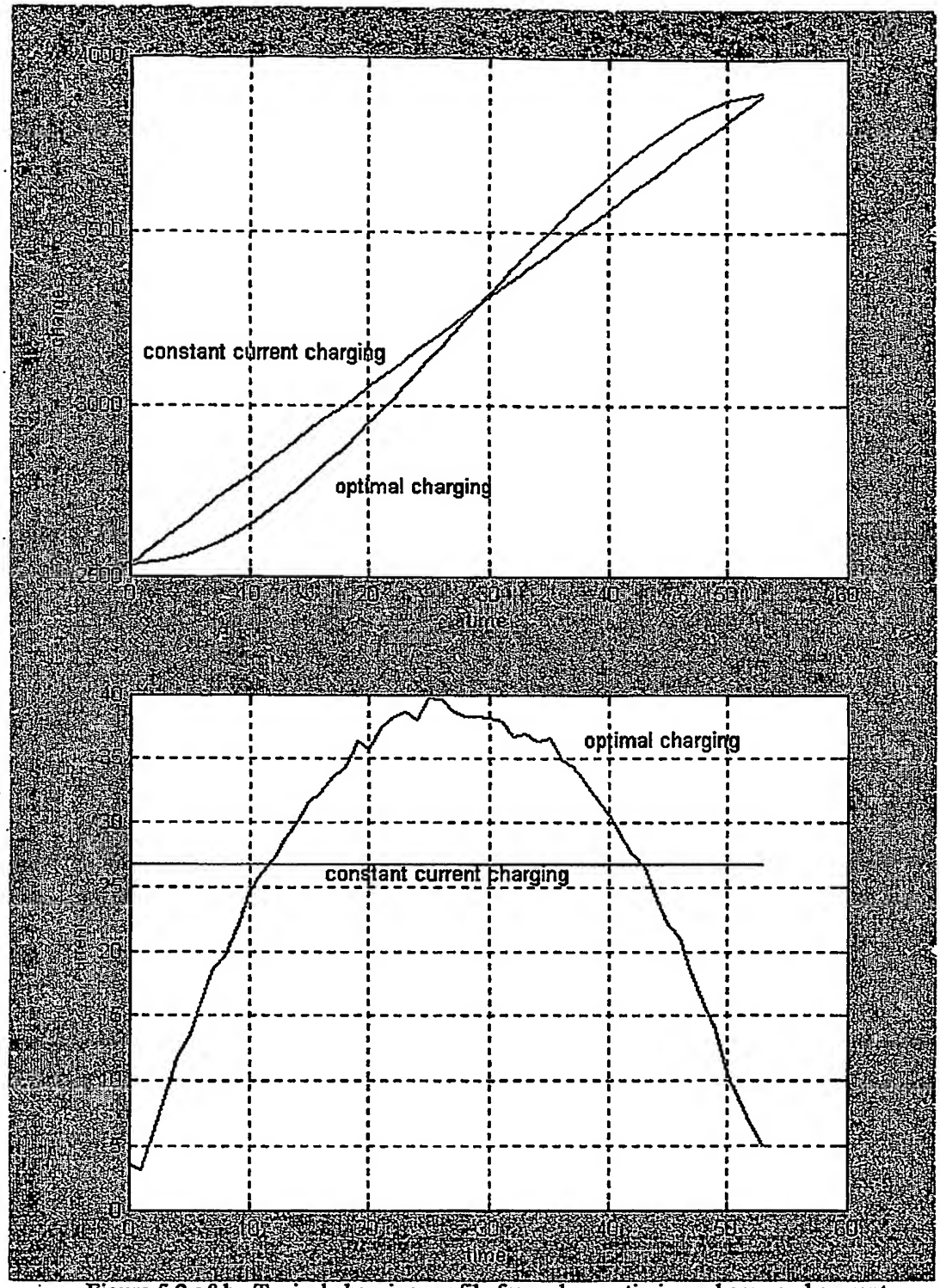

Figure 5.2 a&b. Typical charging profile from slow optimizer, charge and current.

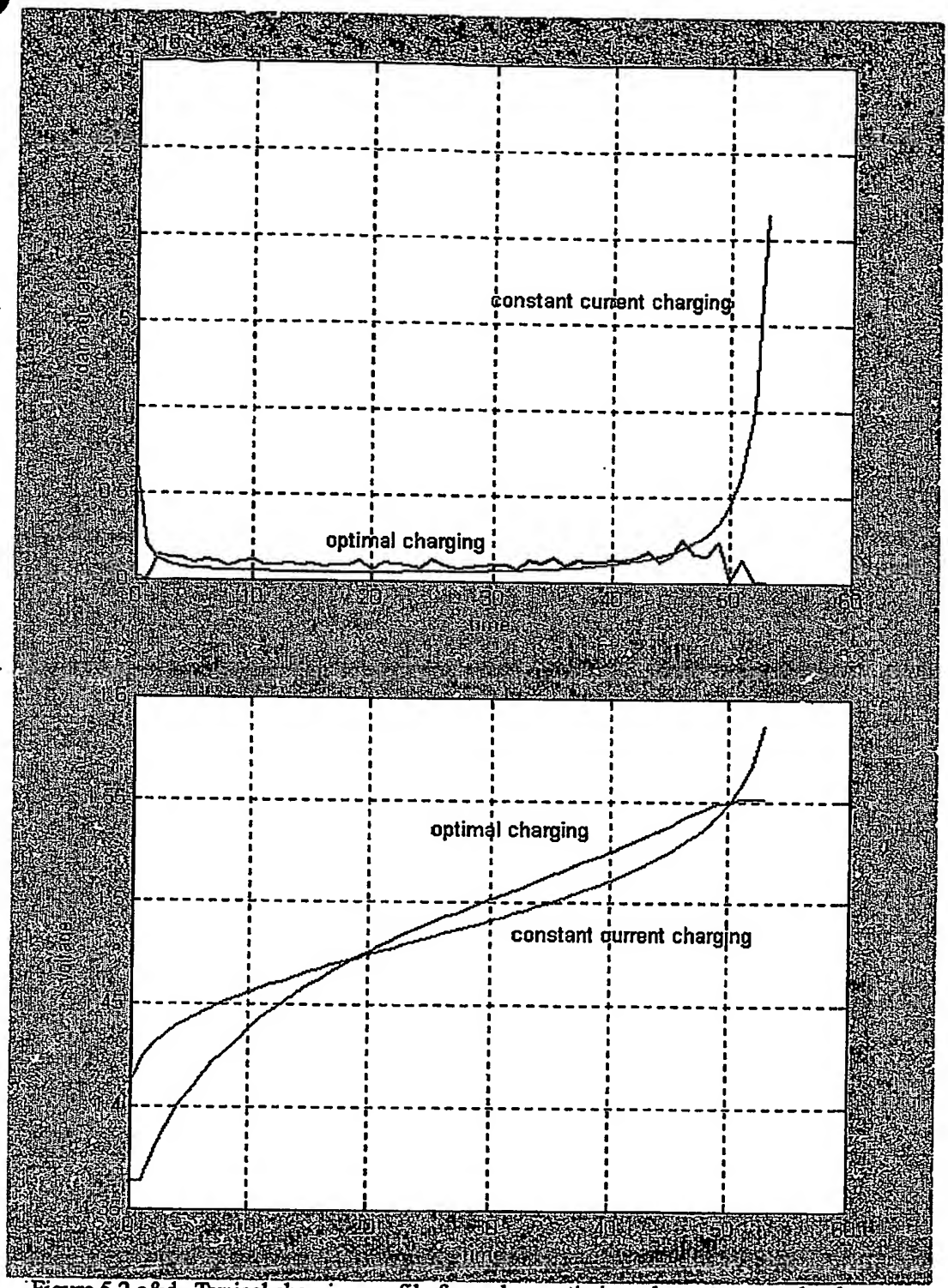

Figure 5.2 c&d. Typical charging profile from slow optimizer, damage rate and voltage.

5.4 Charging Profile Design for Specific Battery

The optimization originally was accomplished by sampling the charging current in time, and optimizing each little sample increment. This optimization approach is very slow and requires many hours of computation time. The results shown in the last section, however, seemed to indicate that the optimal charging profile was similar to a parabola. Using this idea allows a much faster optimization to be accomplished, although the results are probably a little conservative as the truly optimal currents at each point in time are not being calculated. The fast optimization approach is outlined in Figure 5.3. Here a ten point cubic spline is chosen to represent the current profile so as to allow some variation from a parabola (other time functions were also considered which gave similar results). Charging profiles are shown in the next several plots. In performing the optimization, it has been important to be sure to include the cost of requiring the zeroing of a non-zero current at the end of charging, as the large voltage rate there may incur significant damage. Also notice the constant current charge is predicted to last for only 25465 cycles, while the actual cell is still cycling after 50000 cycles. We believe this indicates either some problem with the cycle life data, or that this particular cell has used a design different from that of the cycle life data.

Recognizing that the cell voltage response is diffusion limited on discharge, along with the knowledge that much of the damage occurs near the end of charge when most of the overcharge occurs, allows us to try a charge-discharge profile that backs off from the 100% charged point. Said otherwise, we are going to determine the life-extending charge profile from 60% to 95% fully charged. On discharge, the cell will still use 35% of the AHr capacity since it is diffusion limited at cutoff. On charge, the cell will be kept away from the overcharging region, and thus reduce the damage per cycle. The resulting life-extending control will be implementable in real-time due to the use of an on-board dynamic observer which can keep track of the stored charge material. The use of a real-time observer is discussed in the next section.

The expected improvement associated with the life-extending charge is summarized in Tables 5.1, 5.2, and 5.3 which show a significant potential extension in life expectancy. The percentage life increase should be regarded as approximate due to the use of the fast optimizer and relatively large simulation timestep. It is interesting that the optimal solution using the $|dv/dt|$ term in the damage rate model (Table 5.1 and Figure 5.4), gives the same optimal charging curve as incurring damage only when dv/dt is positive (Table 5.3 and Figure 5.6), although the actual cycle life is different because of different damage rate models.

```
Load previous best
        Guess u(t) function coefficients
        Initialize simulation
            Main simulation loop
                        Derivative function evaluations
                        Numerical integration (Euler, T=1)
                        Damage rate calculation
                        Integrate damage rate
            End main loop
            Include final state error into Performance Measure
    Change u(t) function coefficients using gradient search and repeat until optimal
Store present best
```

Figure 5.3 Outline of fast optimization approach.

	Damage per Cycle	Cycles to Failure	Life-extending-Charge		% Life Extension
			Damage per 65-100% Cycle	Cycles to Failure	
Constant-Current Charge	3.9269e-005	25465	2.0780e-005	48123	88.98%
Constant + Taper Charge	2.6316e-005	38000	2.0780e-005	48123	26.64%

Table 5.1 Life-extending charge compared to constant current and constant current + taper.

	Damage per Cycle	Cycles to Failure	Life-extending-Charge		% Life Extension
			Damage per 60-95% Cycle	Cycles to Failure	
Constant-Current Charge	3.9269e-005	25465	1.9535e-005	51190	101.02%
Constant + Taper Charge	2.6316e-005	38000	1.9535e-005	51190	34.71%

Table 5.2 60%-95% Life-extending charge compared to constant current and constant current + taper.

	Damage per Cycle	Cycles to Failure	Life-extending-Charge		% Life Extension
			Damage per 65-100% Cycle	Cycles to Failure	
Constant-Current Charge	3.9269e-005	25465	2.2080e-005	45290	77.85%
Constant + Taper Charge	2.6316e-005	38000	2.2080e-005	45290	19.18%

Table 5.3 Life-extending charge compared to constant current and constant current + taper using only positive dv/dt in the damage rate law..

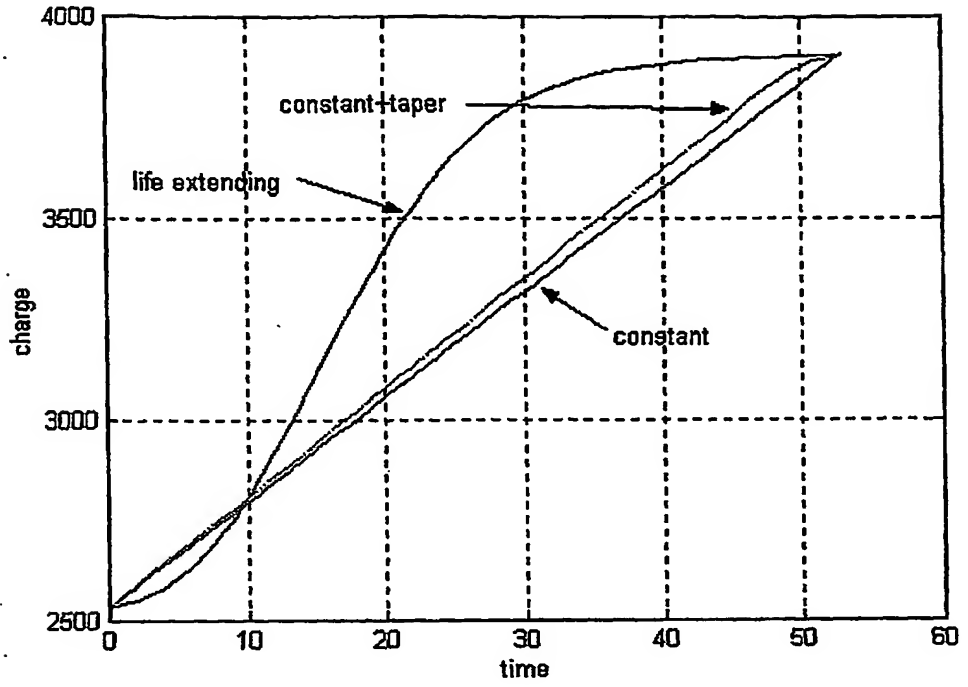

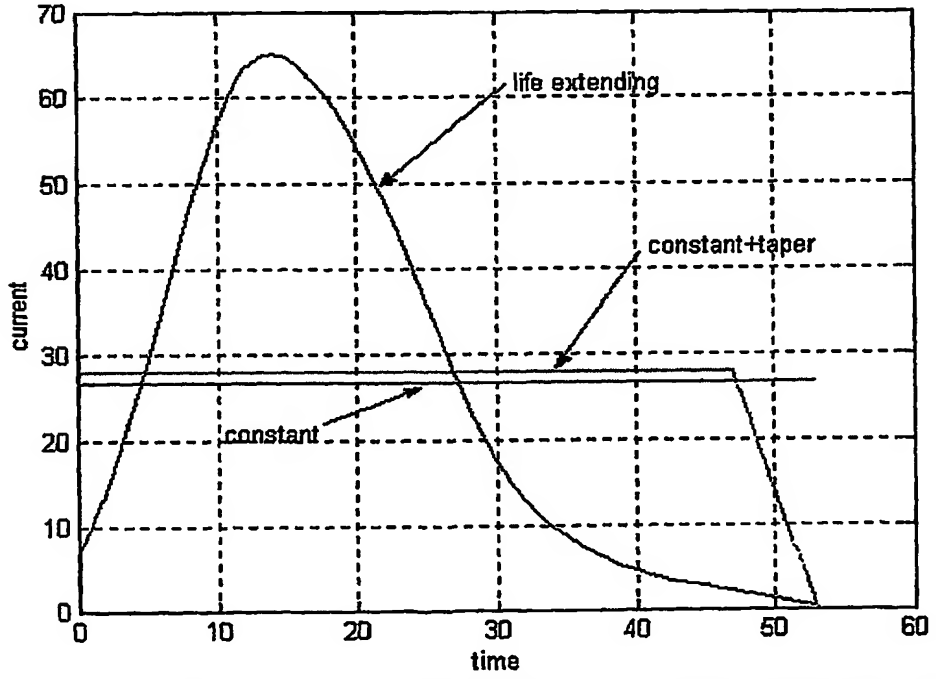

Figures 5.4a&b. Comparison of 65%-100% charging methods, charge and current.

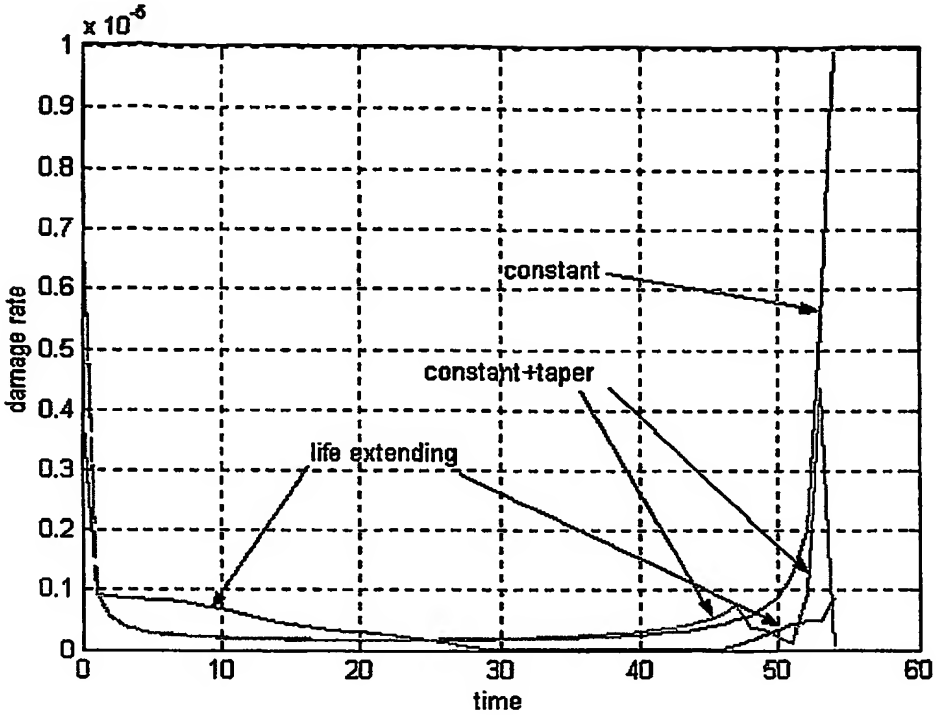

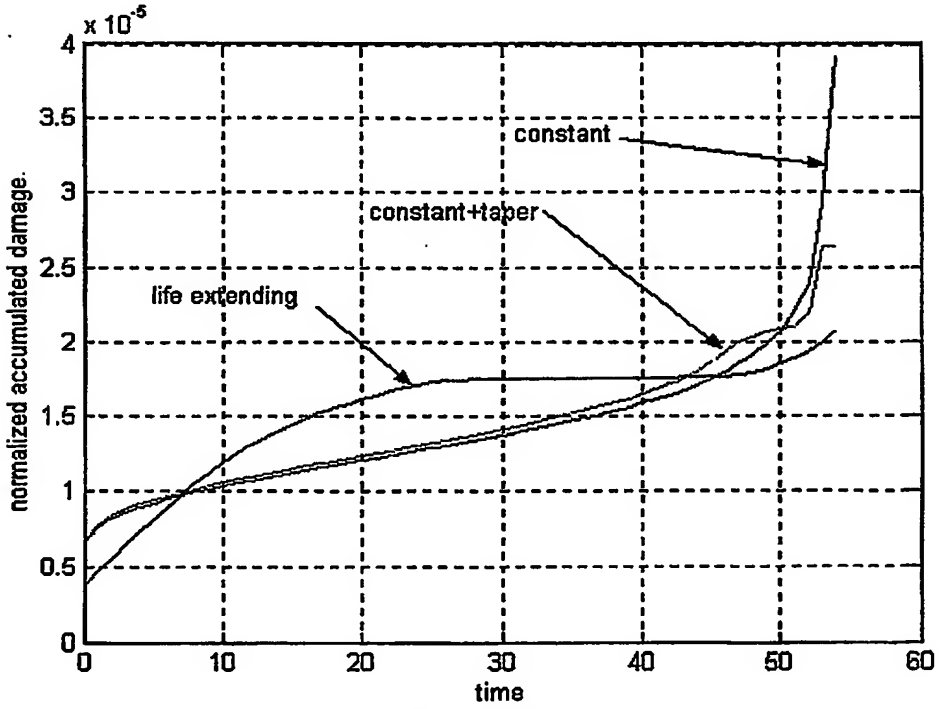

Figures 5.4 c&d. Comparison of 65%-100% charging methods, damage rate and damage.

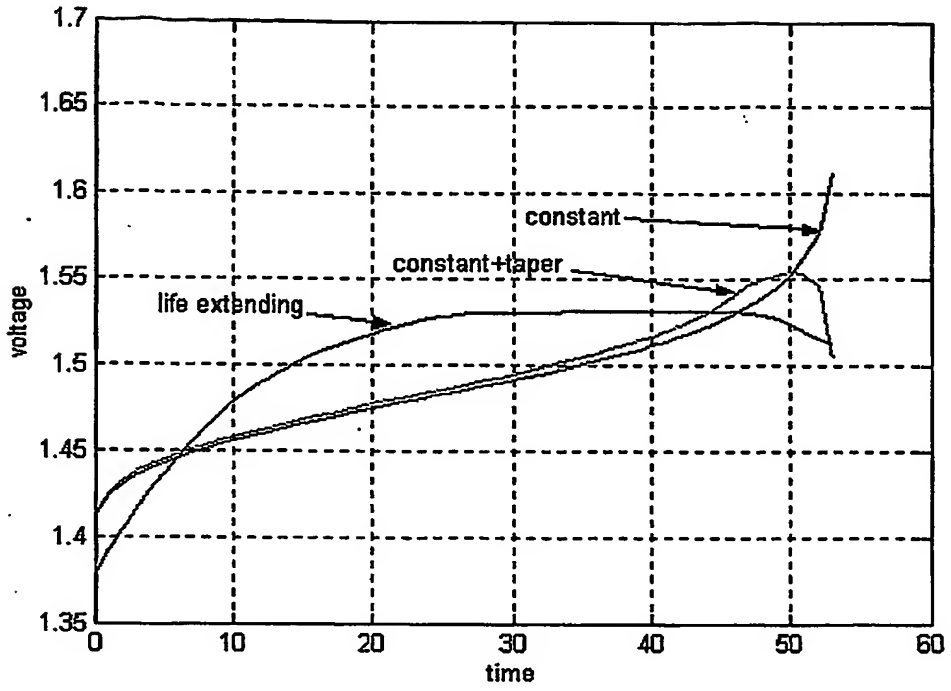

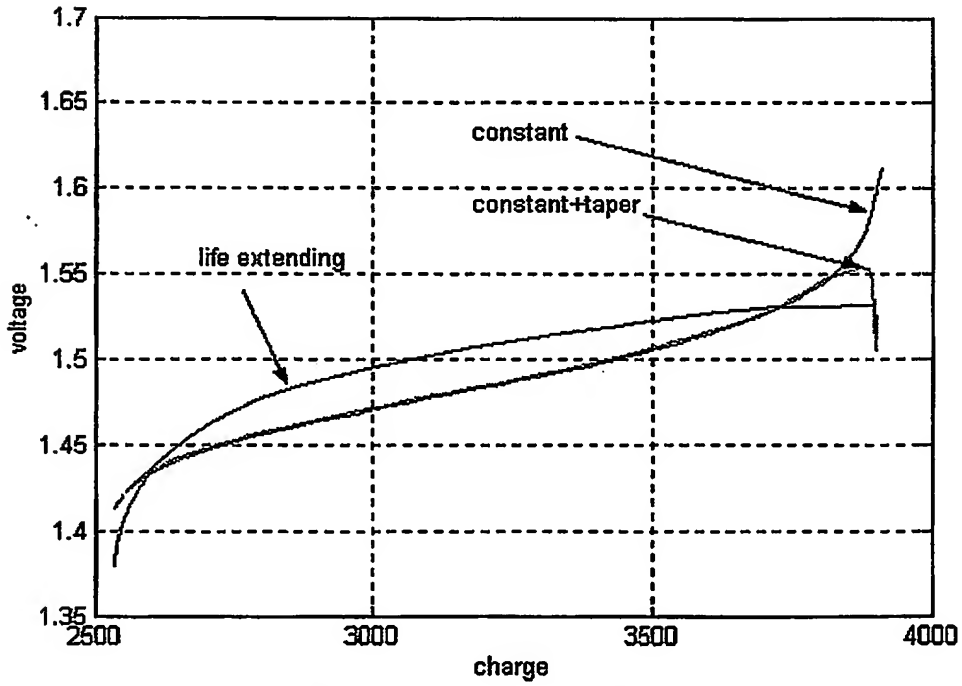

Figures 5.4 e&f. Comparison of 65%-100% charging methods, voltage.

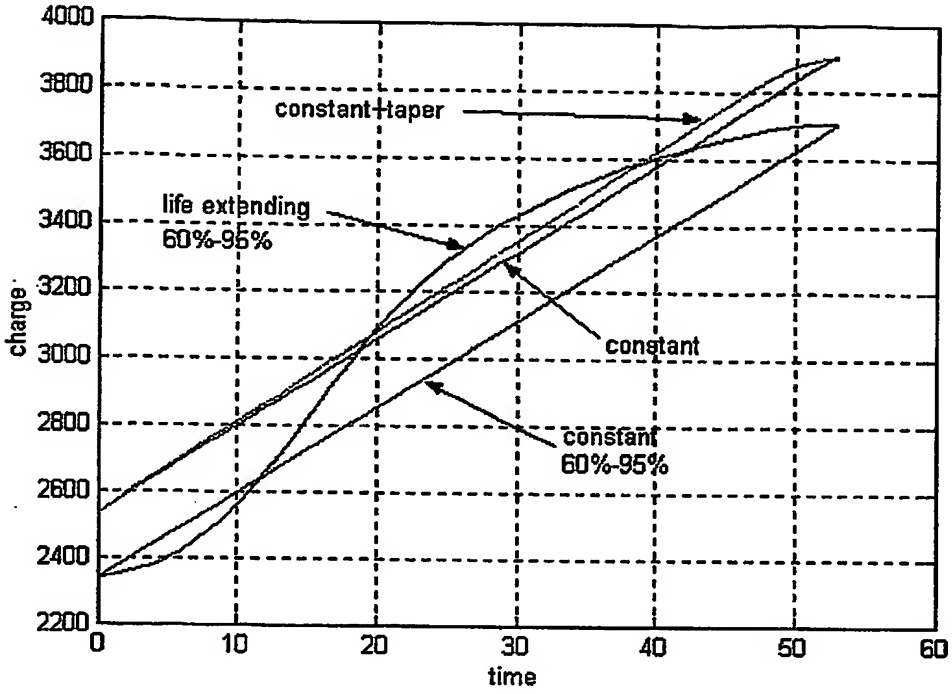

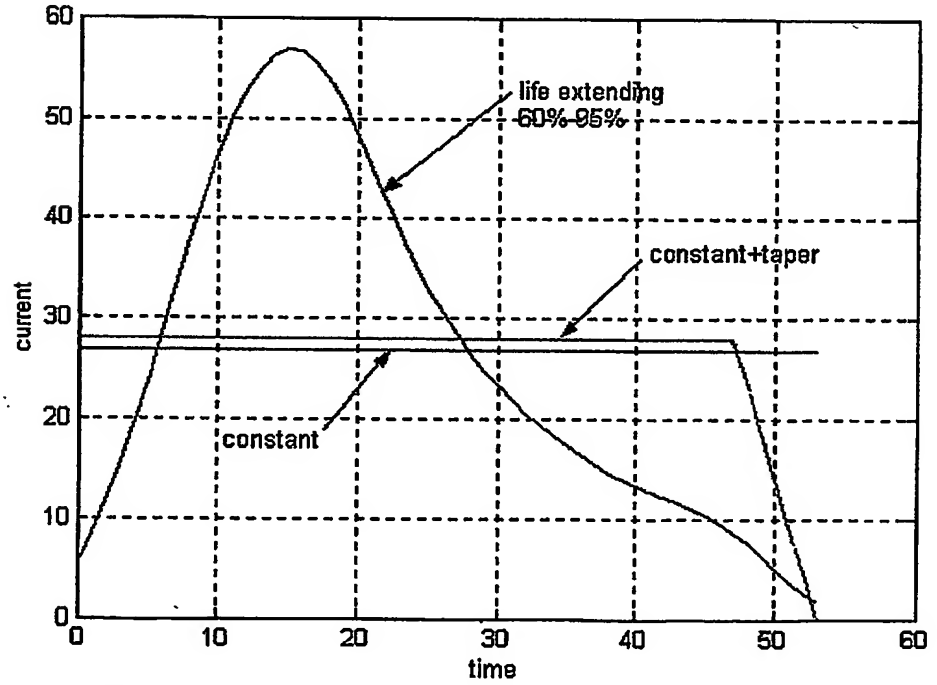

Figures 5.5 a&b. Comparison of 60%-95% and standard charging methods, charge and current.

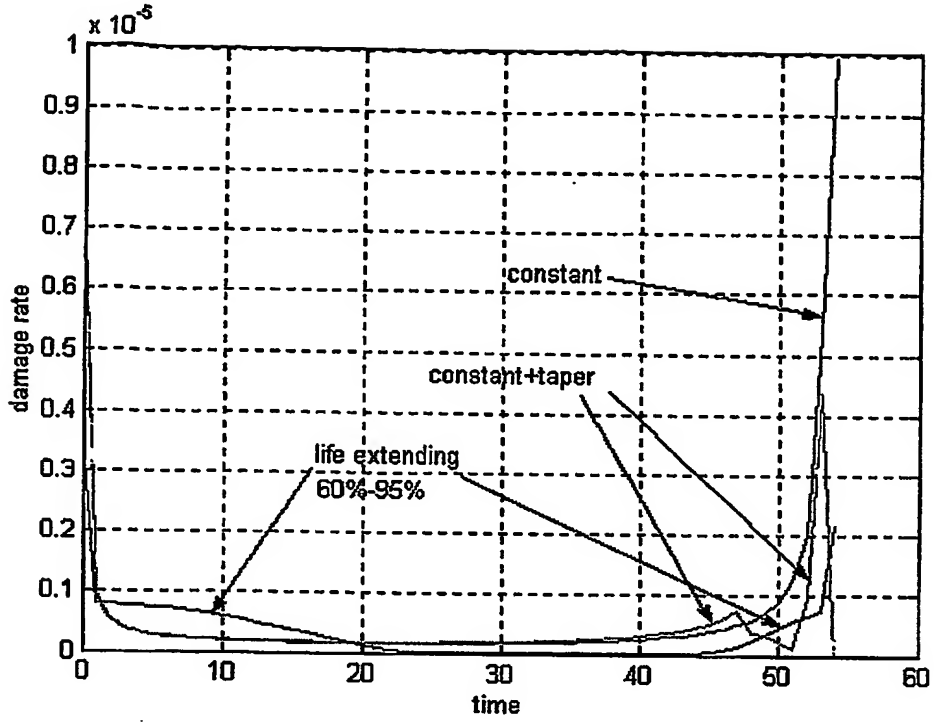

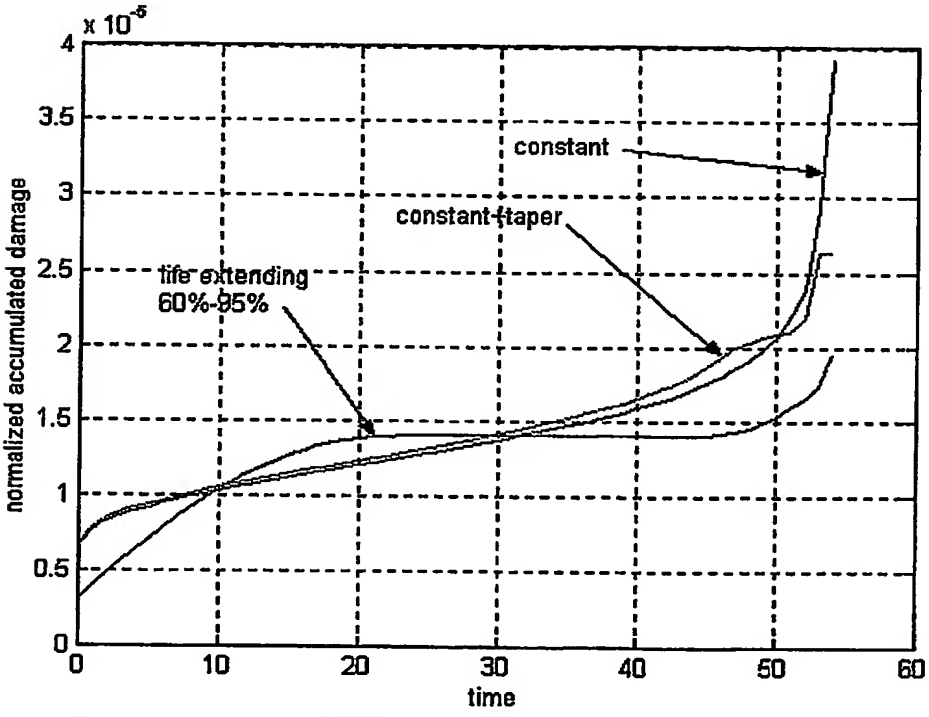

Figures 5.5 c&d. Comparison of 60%-95% and standard charging methods, damage rate and damage.

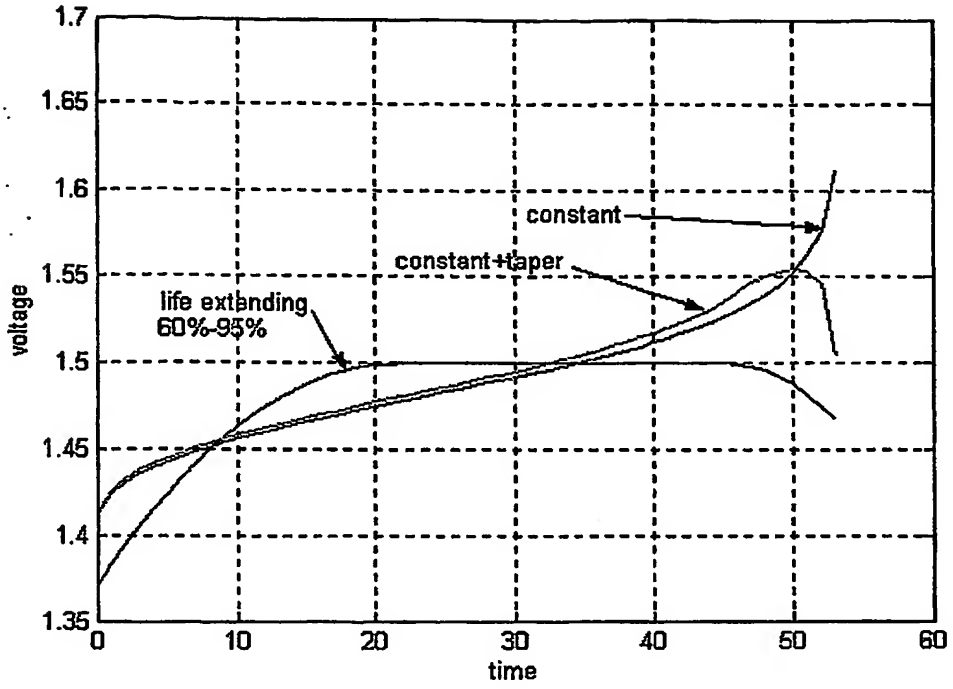

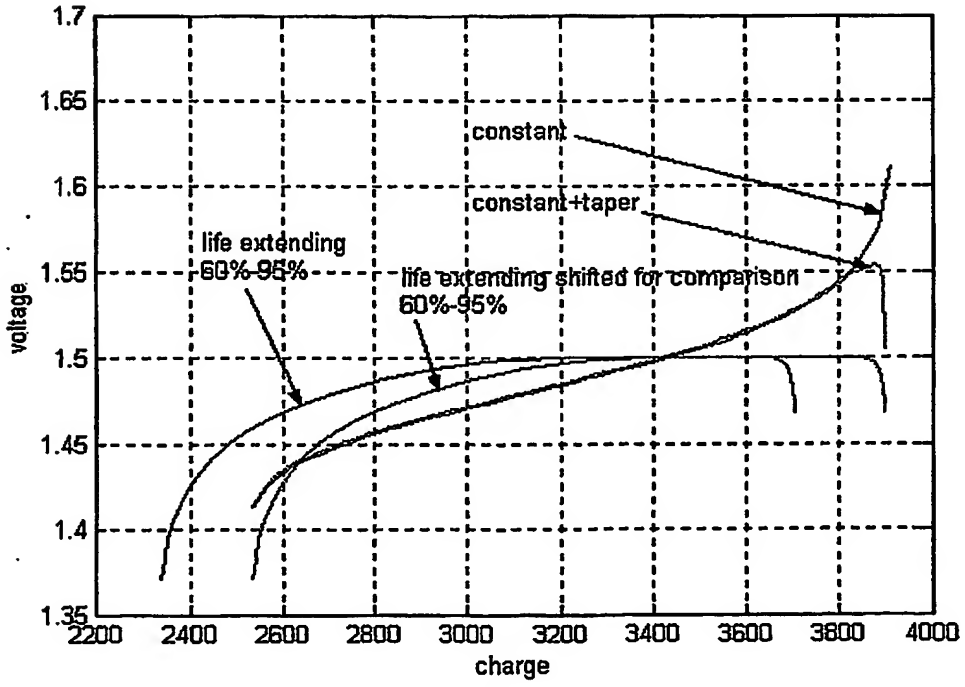

Figures 5.5 e&f. Comparison of 60%-95% and standard charging methods, voltage.

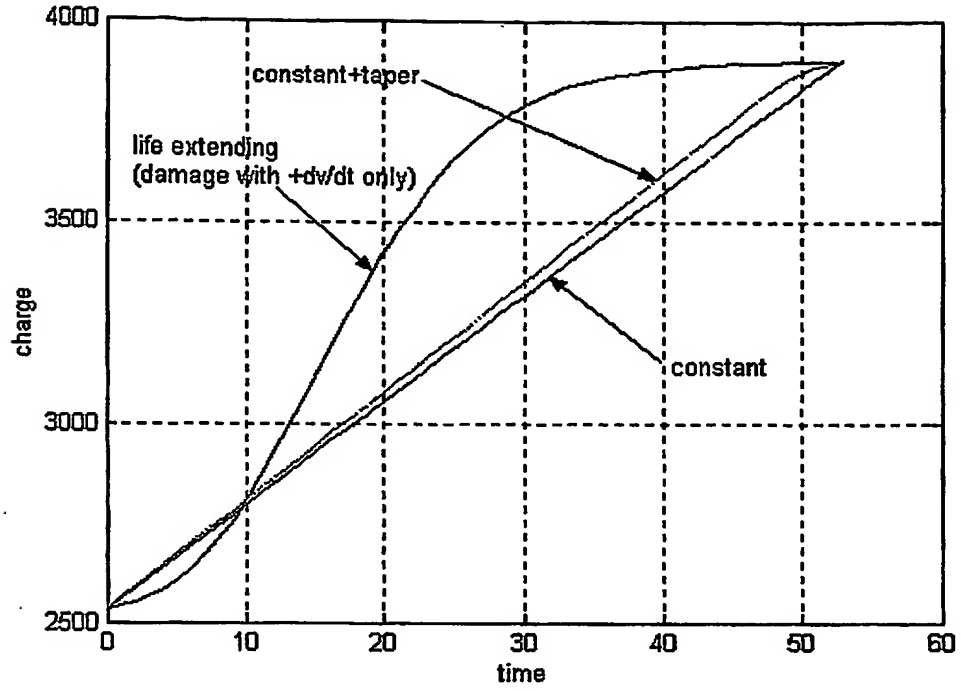

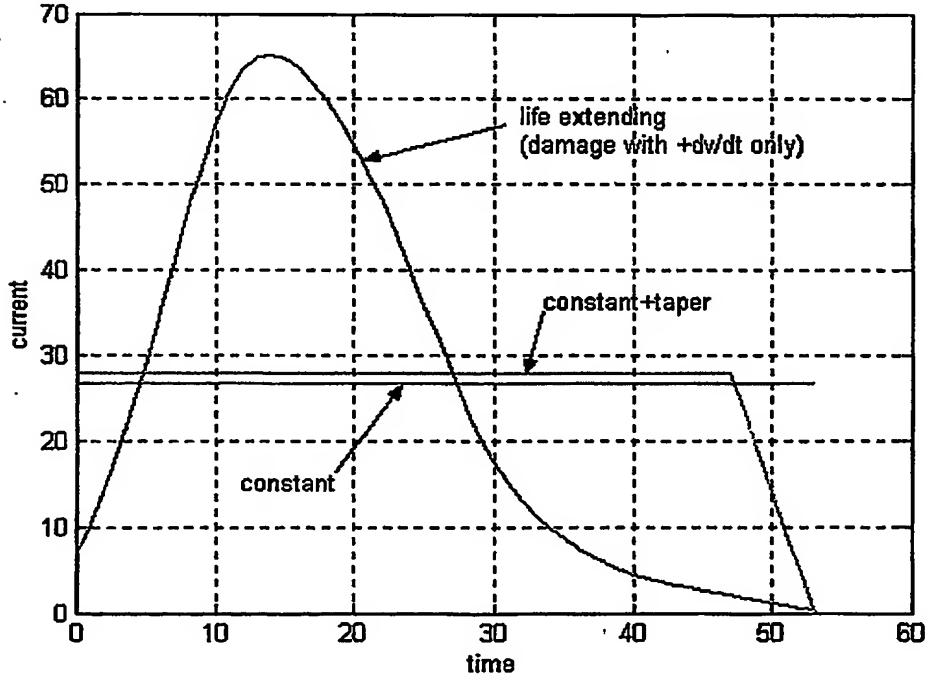

Figures 5.6 a&b. Comparison of life extending (+dv/dt damage only) and standard charging methods.

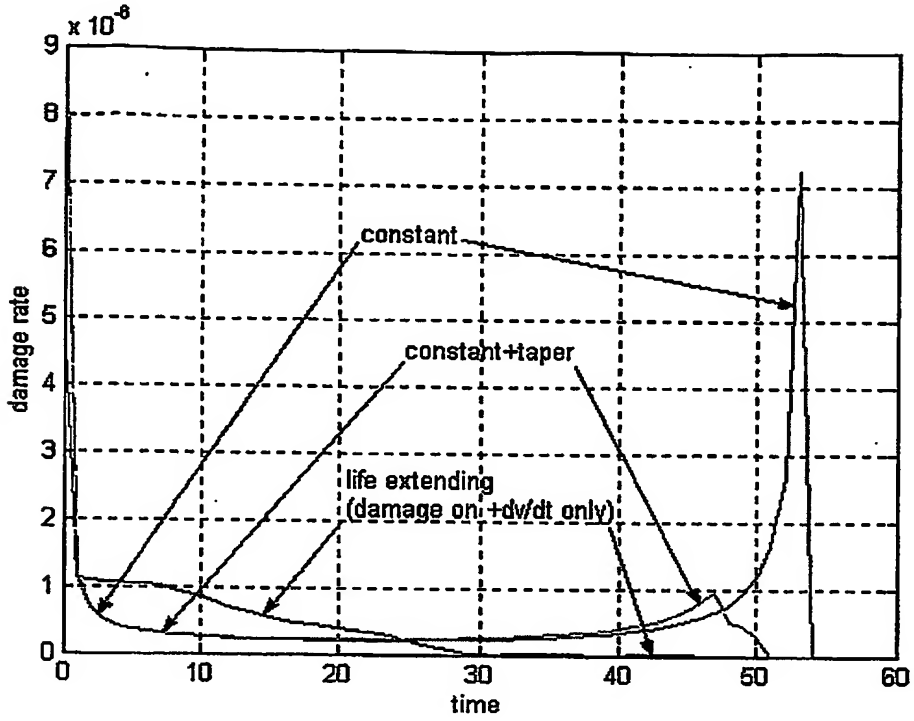

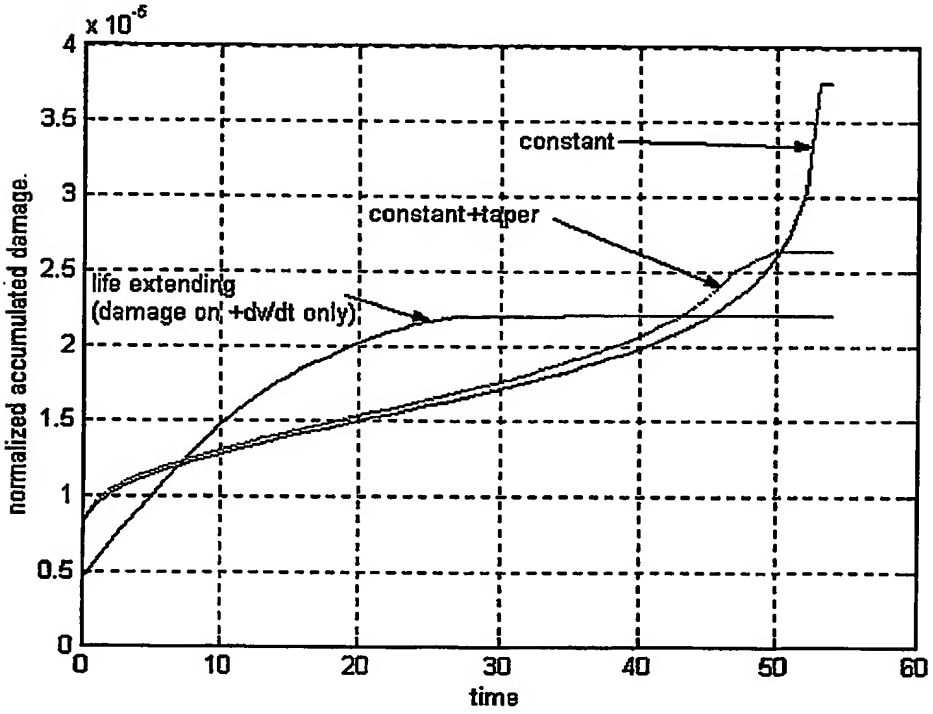

Figures 5.6 c&d. Comparison of life extending (+dv/dt damage only) and standard charging methods.

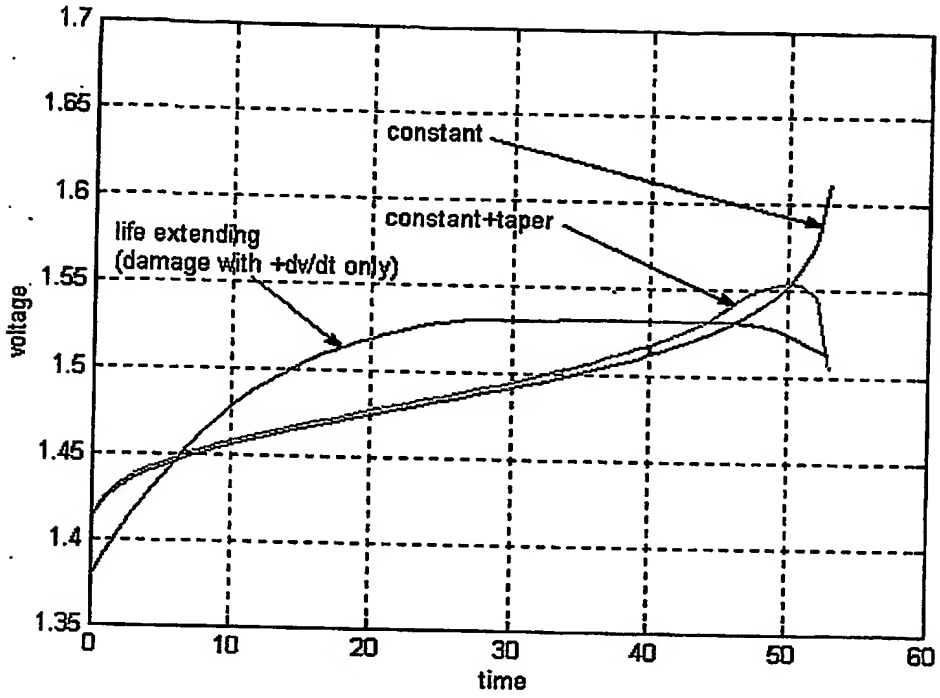

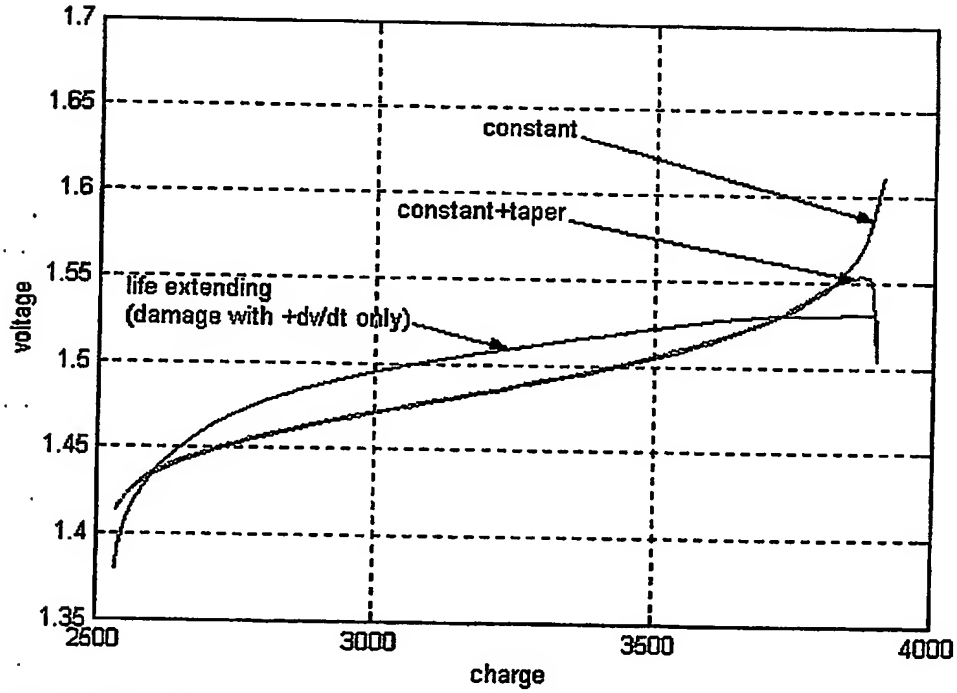

Figures 5.6 e&f. Comparison of life extending (+dv/dt damage only) and standard charging methods.

6.0 Suggested Real-time Implementation

6.1 Real-time Observers

An important result of state space control theory is the concept of a state observer (Luenberger (1971)). The total number of dynamic "states," or "state variables," in a system is equal to the number of energy storage elements in the system, which is also equivalent to the number of time derivatives that are needed in the differential equations representing that system (Freidland(1986)). The "state" of a given system is the collection of all the "state variables" of that system at a given point in time. This collection is all the information needed to advance the "state variables" forward in time through the differential equations representing the system. With these definitions, the concept of a state observer will now be clarified.

A state observer is effectively a dynamic model of a given system that runs in real-time, and in parallel with the actual system. Typically, only a small number of the dynamic states of an actual system are measureable, or are sensed. In the case of an electrochemical cell, typically only terminal voltages and currents, and perhaps some pressures and temperatures are all that are sensed. The state observer is then used to provide an estimate of the non-sensed variables. There are usually two forms for state observers, the open-loop observer and the closed-loop observer.

An open-loop observer receives the same inputs as the actual system, and then provides the collection of dynamic states as an output (Jacquot(1981)). If the model being used in the observer is accurate, then all the dynamic states from the observer will accurately represent the true states in the actual system. This has been applied successfully to a jet engine (Merrill and Lorenzo (1988)), as well as other places. A closed-loop observer receives the same inputs as the actual system, as well as all of the sensed dynamic states and outputs from the actual system (Jacquot (1981)). Comparing these sensed variables with the corresponding simulated variables, the difference can be used as a feedback signal to force the observer dynamic states to converge to the true dynamic states of the actual system (see Figure 2). This approach does not require the model to be as accurate as in the open-loop observer due the correction of the feedback from the sensed variables. Closed-loop observers are used in most state space control designs (Maciejowski(1989), Stengel (1986)), where they have also been used to filter noise out of the measurements.

A real-time observer for an electrochemical cell incorporates the hybrid cell model, as discussed in the previous section, into a microprocessor based simulation that would be required to run in real-time. Sensed variables from an actual cell would then be input to the microprocessor simulation to force the dynamic states of the real-time cell observer (simulation) to converge to the corresponding states in the actual cell. The feedback is crucial for this problem as the actual system is highly nonlinear as well as spatially distributed, and the model dynamic states represent aggregations of many actual states. Even so, the feedback to the observer will force the errors in the measured variables to zero, and the unmeasured variables will accurately represent the corresponding actual variables (Krob (1992)). It is expected that a real-time observer for an electrochemical cell will be able to provide accurate information about state of charge, active species concentrations, and internal temperature. Any theory required for the fractional order components in the observer will need to be developed. More advanced observer designs may also provide some indication of damage as discussed below.

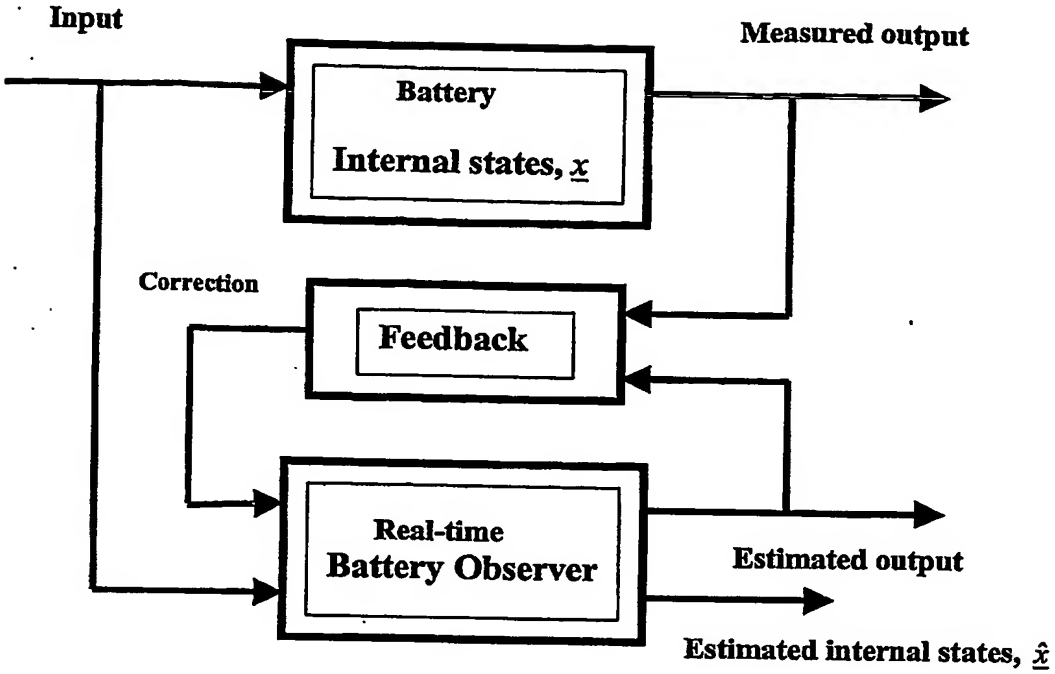

Figure 2. Real-time observer structure.

6.2 Observer Based Control

Typically real-time observers are used in two ways, for continuous-state feedback and for decision making. Much of modern control theory is based on state feedback. State feedback requires knowledge of all the dynamic states of the given system, which are then fed back to the system inputs to improve overall system performance. As most of these dynamic states are not measurable, most state feedback controllers use the estimated states from real-time observers for feedback purposes.

Observers can also be used as part of the general decision making process. To do so, then requires an extra layer of intelligence. For example, if the observer predicts that certain dynamic states have varied too far from where they are supposed to be, the higher level of intelligence can determine if some sensors have failed, if some actuators have failed, or if the actual system has become damaged in some way (Merrill and Lorenzo (1988)). Of course, this intelligent layer must be programmed by a knowledgeable user. Another decision making application could be to shut the system down if certain observed dynamic states exceeded those which would normally be deemed healthy for the actual system. These decision making control strategies will be addressed later when discussing advanced controllers and life-extending control.

Some of the issues associated with observer based control of batteries and fuel cells require a clear understanding of improved performance. Some potential definitions of improved performance might include maximum energy out, maximum power out, constant voltage out, constant current out, constant power out, prolonging state of health, or minimum damage rate, among others. Other issues are more hardware related. For example, in a collection of cells, control of each cell would probably be important. An array of observers,

one for each cell, would then be able to provide information about individual cells. As long as each cell could be independently controlled, this information could actually be used handle any degradation or failures of individual cells. Of course this also requires the usage of power electronics to control the charging and discharging of individual cells (Tarter (1993)). This could include the use of buck-boost DC-DC converters to provide constant voltages or currents out, as cell voltages and states of charge change. Finally, any theory necessary for control of the fractional order components will be developed.

6.3 Advanced Real-time Observers

An advanced real-time observer for electrochemical cells would require an extra level of intelligence over the standard real-time observer. Specifically, the algorithm used for the identification of the cell hybrid-model parameters would need to be automated (Goodwin and Sin(1984)). This would then allow two things. First, it would allow the tracking of parameters as a cell changes during its lifetime. Some knowledge of parameter range could indicate when a cell was nearing failure. Second, it would allow the on-line determination of the cell model parameters to begin with, or effectively, the correction of the initial parameters provided to the real-time observer. Effectively, the real-time observer could then "learn" any battery. An advanced real-time observer should also include models of any damage mechanisms as a function of the system states.

It is felt that degradation algorithms should be included into an observer structure to give a real-time damage indicator for a given cell (Tobias and Trindale (1995)).

6.4 Advanced Controllers

An advanced controller for an electrochemical cell would also require an extra level of intelligence. Specifically, the advanced controller would use the information provided by the advanced real-time observer to maintain cell performance as the cell's parameters change with time. This would require a continuous change of controller gains as the effect of physical changes in a given cell were updated by the advanced real-time observer (Goodwin and Sin(1984)).

Secondly, an advanced controller would need to implement some of the decision making skills as discussed earlier in the Observer Based Control section. If the estimates provided by the real-time observer vary too much from the actual cell outputs, then decisions would be required concerning sensor, actuator, or cell health. If any failures were detected, additional intelligence would be required to accommodate a detected failure. Of course, the chosen battery and control structure must allow accommodation.

Finally, assuming some form of a damage model was available, the controller could then make performance-lifetime trade-off decisions. Associated with this intelligence, there may need to be off-line optimization studies performed that determine the most efficient charging (or discharging) profile which will also prolong the cell lifetime. This is related to the area of optimal control. One of the most well known off-line optimal control results is the minimum-time-to-climb jet fighter intercept solution which was not at all expected (Bryson and Ho(1975)). Another example of off-line optimization results is the reusable rocket engine damage mitigating control mentioned earlier (Lorenzo (1992)). Ultimately, designing a cell charging (or discharging) profile that extends the useful life of the cell by minimizing accumulated damage would be a useful result.

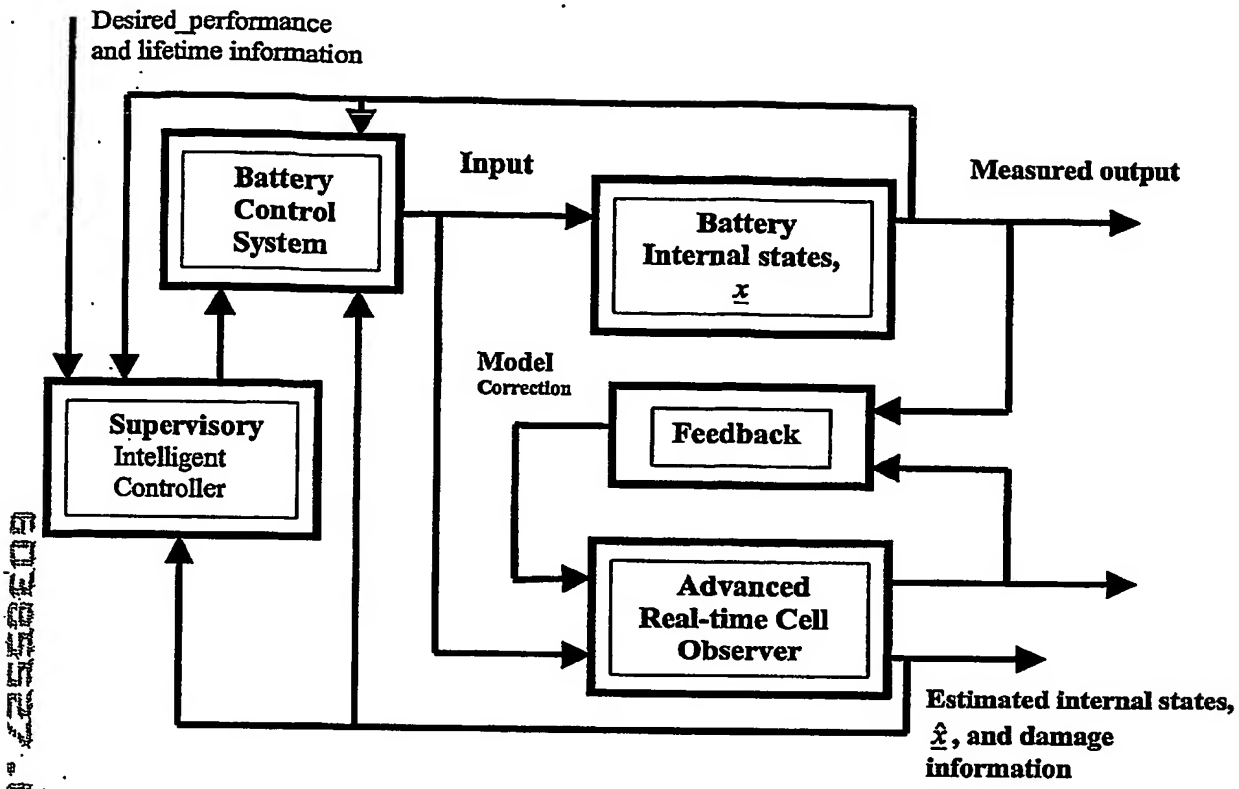

Figure 3. Advanced control system using advanced real-time observer.

7.0 Summary and Future Research

7.1 Summary

In this report, we have presented a methodology for extending the life of NiH2 cells via a damage-mitigating charging current. This has required the development of an essentialized dynamic model that will accurately reconstruct internal states in a given cell. The parameters of this model are readily obtainable from either off-line data, or adaptively on-line from real-time data. To determine the life-extending charging current, an instantaneous damage model that determines the damage rate at any point in time based on voltage measurements, has been developed. Using the instantaneous damage rate model with the essentialized cell model, allows the development of a the damage mitigating charge profile for extending the life of the cell. This charge profile is obtained via optimization, and can be modified by trading recharge for damage. Once the life-extending charge profile has been obtained, the implementation of this profile is performed via a real-time controller that uses a real-time observer for reconstructing the internal cell variables based on current and voltage measurements at the cell terminals. This real-time controller implementation can be used over the entire life of the cell by updating any combination of the model parameters, control parameters, or charging profile based on the data from the present charge-discharge cycle.

<u>Model Development</u>

1. Developed an essentialized NiH2 cell model structure.
2. Developed a method for determine the essentialized model parameters for charge-discharge data.
3. Developed a deeper understanding of the charge-discharge hysteresis behavior in the voltage-charge plane.

<u>Damage Model</u>

1. Developed an instantaneous damage model for NiH2 cells based on cell voltage measurements.
2. The instantaneous damage rate is shown to depend on voltage and voltage rate.
3. It is shown that the size of the voltage-charge hysteresis curve is related to the damage per cycle.

<u>Life-extending Charge Development</u>

1. A life-extending charging profile has been developed by optimizing the charging current with respect to the damage per cycle and total recharge.
2. This life-extending current should provide significant life extension over the present recharging methods.
3. Significantly more life extension for a given cell can be obtained by not recharging the cell to 100%.
4. Some heuristic rules for minimum damage charging that have emerged are:
   a. Increase the charging current slowly at the beginning of charge.
   b. Put more of the charge in during the first half of charging.
   c. Decrease the current to zero slowly at the end of charge.
   d. During charge, try not to allow the terminal voltage to increase much beyond the thermoneutral voltage.
   e. Try to keep the voltage-current hysteresis-curve area as small as possible.

Observer Development

1. A fractional-order observer theory (necessary for control implementation of the model) has been developed.
2. A parameter identification technique is discussed for allowing a real-time essentialed model to track changes in its parameters in real-time over the life of a cell.
3. A tracking controller for implementing the optimal charging profile in real-time based on observed system states is discussed.
4. A learning controller that continuously updates the charging profile based on changing cell parameters has been discussed.

7.2 Future Diections

Overcharge Control

It is noted that H2 pressure seems to be related to overcharge, and thus to damage. By monitoring the H2 pressure in a NiH2 cell, it should be possible to provide some control for overcharging. The cell pressure was not included in our essentialized model, but could be without much increase in complexity. We could then relate then H2 pressure to both overcharge and damage.

By using our instantaneous damage model, both a real-time damage rate sensor and an on-line damage monitor could be developed. The damage rate sensor would require knowledge of the amount of stored material, and the present voltage. The damage monitor, or life predictor, could be developed using the damage rate sensor, or by using an accelerated degradation model as discussed in Tobias and Trindade.

Ultimately a charge-discharge controller could use feedback from these sensors to trade-off lifetime with performance.

Other Chemistries and Fuel Cells

It is expected that this methodology can be readily applied to other chemistries, such as Li-based cells if cycle-life data is available. If this data is not available, a cycle-life model can be inferred from an accelerated degradation approach (Tobias and Trindade).

With regard to fuel cells, this methodology should also be applicable, however it will be necessary to modify the essentialized model structure for the two fuel sources. It will also be necessary to understand the damage mechanisms associated with fuel cells. Alternatively, it is expected that a tracking controller should be able to immediately improve performance in a fuel cell.

Discharge Damage Control

Although discharge control was considered outside the scope of this research, various possibilities exist to reduce damage during the discharge part of the cycle. It was assumed in the damage modeling that the entire damage during the cycle took place over the charging part of the cycle. It is of course possible to apportion that damage over both the charge in the discharge parts of the cycle. In the former, the damage model is dictated by the form of the damage per cycle and would remain very much the same. Future research could generalize the damage model to include damage on both charging and discharging. With the availability of the generalized damage model, various strategies could be investigated which would control damage during

discharge. The additional aspect of such research is that it could influence the manner in which the battery power is allocated. The acceptability of this would depend on the specific application.

Damage Testing and Future Data Needs

The present research allowed access to the Crane database. From our observation of the database, which is certainly not a detailed analysis of the database, we have found it to be an excellent resource for evaluation of battery designs and battery chemistries, etc. However, it was not clear that appropriate data was available in the database, for evaluating and creating damage models for particular battery types. It has been our observation, that in some of the battery literature, the battery design aspects and the battery operational aspects are not clearly delineated. It is important to separate these two areas, and to develop as a separate discipline, battery operational theory. In particular, clean operational data seems to be required. By this we mean tests to failure, with key parameters held constant. One direction of future research would be to establish testing methods specific to obtaining usable damage (operational) models. This involves accurate assessment of the equation forms for cycle damage as well as proper statistical treatment of the data.

8.0 References

Bard, Allen J. and Faulkner, Larry R. (1980), Electrochemical Methods, Wiley, New York.

Briton, Doris L. and Miller, Thomas B. (2000), "Battery Fundamentals and Operations: Batteries for Dummies," internal publication, Electrochemistry Branch, NASA Glenn Research Center.

Bryson, Jr., A.E. and Ho, Y.C. (1975), Applied Optimal Control, Hemisphere, New York.

Buder, E. (1972), "Oxygen evolution during recharging of positive nickel oxide sinter electrodes," J. of App. Electrochem., vol. 2, pp 301-308.

Chicatelli, Amy, and Hartley, Tom T. (1998), "A Method for Generating Reduced-Order Linear Models of Multidimensional Supersonic Inlets," NASA CR-1998-207405, May 1998.

Dorf, Richard C. (1974), Modern Control Systems, Addison-Wesley, Reading.

Doyle, Marc, Fuller, Thomas F., and Newman, John (1993) "Modeling of Galvanostatic Charge and Discharge of the Lithium/Polymer/Insertion Cell," J. Electrochem. Soc., vol 140, no 6, pp 1526-1533, June 1993.

Friedland, Bernard (1986), Control System Design, McGraw-Hill, New York.

Goodwin, G.C. and Sin , K.S. (1984), Adaptive Filtering Prediction and Control, Prentice-Hall, Englewood Cliffs.

Green, R. (1991), "Detailed Battery Life Procedure/Assumptions," internal NASA Glenn Reseach Center Electrochemistry Branch document.

Hartley, Tom T., Beale, Guy O. and Chicatelli, Stephen P. (1994), Digital Simulation of Dynamic Systems, Prentice-Hall.

Hartley, Tom T., Veillette, Robert J, DeAbreu-Garcia, . J. Alexis, Chicatelli, Amy, and Hartmann, Richard (1998), "To Err is Normable: The Computation of Frequency Domain Error Bounds From Time Domain Data," NASA CR-1998-208516.

Jacquot, Raymond J. (1981), Modern Digital Control Systems, Marcel-Dekker, New York.

Krob, Robert (1991), "A Real-time Observer for A Continuous-casting Process," M.S. Thesis, Department of Electrical Engineering, The University of Akron.

Linden, David (1995), Handbook of Batteries, McGraw-Hill, New York.

Lorenzo, Carl F., Saus, J. R., Ray, A., Carpino, M. and Wu, M. K. (1992), "Life Extending Control for Rocket Engines,", NASA-TM-105789, August 1992.

Lorenzo, Carl F. (1994), "Continuum Fatigue Damage Modeling for Use in Life Extending Control," NASA TM-106691, August 1994

Lorenzo, Carl F. and Hartley, Tom T. (1998), "Initialization, Conceptualization, and Application in the Generalized Fractional Calculus," NASA TP-1998-208415.

Luenberger, D. (1971), "An Introduction to Observers," IEEE Trans. Auto. Cont., AC-16(6), pp 596-602, December 1971.

Maciejowski, J.M. (1989), Multivariable Feedback Design, Addison-Wesley, Wokingham, England.

Merrill, Walter, and Lorenzo, Carl F. (1988), "A Reusable Rocket Engine Intelligent Control," 24th Joint Propulsion Conference, Cosponsored by AIAA, ASME, and ASEE, Boston MA, July 1988.

Newman, John S. (1991), Electrochemical Systems, Prentice-Hall, USA.

Sanabria, Olga D. Gonzales-, "Effect of NASA Advanced Designs on Thermal Behavior of Ni-H2 Cells," internal NASA Glenn Reseach Center Electrochemistry Branch document.

Shepherd, Clarence M. (1965), "Design of Primary and Secondary Cells, I," J. Electrochem. Soc., vol 112, no 3, pp 252-257, March 1965, and "Design of Primary and Secondary Cells, II," J. Electrochem. Soc., vol 112, no 7, pp 657-664, July 1965.

Stengel, Robert F. (1986), Stochastic Optimal Control, Wiley, New York.

Sun, H.H., Abdelwahab, A.A., Onaral, B. (1984), "Linear Approximation of Transfer Function of Pole of Fractional Order," IEEE Trans. Auto. Cont., vol. 29, no. 5, pp.441-444, May, 1984.

Tarter, Ralph E. (1993), Solid State Power Conversion Handbook, Wiley, New York.

Tobias, Paul A. and Trindade, David C. (1995), Applied Reliability, 2nd, Chapman & Hall/CRC, Boca Raton.

Xia, Lei and Hartley, Tom T. (2000a), " Device Characteristics of Batteries and Fuel Cells," 17th International Electric Vehicle Symposium, October 2000.

Xia, Lei and Hartley, Tom T. (2000b), "Behavioral Modeling of Batteries and Fuel Cells," 2000 Power Systems Conference, November 2000, San Diego.

CLAIMS FOR UA.439P ENTITLED OPTIMAL BATTERY CHARGING FOR DAMAGE MITIGATION

What is claimed is:

1. A method for charging an electrical storage device so as to extend the life thereof, comprising:

developing an essentialized cell model structure of the electrical storage device;

determining model parameters for charge-discharge data of said structure; and

determining charge-discharge hysteresis behavior of said structure in a voltage-charge plane.

2. The method according to claim 1, further comprising:

measuring voltage values of said structure based upon said charge-discharge hysteresis; and

deriving an instantaneous damage rate from said measured voltage values.

3. The method according to claim 2, further comprising:

developing a charging profile based upon said instantaneous damage rate, wherein said charging profile optimizes a charging current with respect to the damage per cycle so as to extend the overall life of the electrical storage device.

IN THE UNITED STATES PATENT AND TRADEMARK OFFICE

In the application of

TOM T. HARTLEY and
CARL F. LORENZO

Serial No.

Filed

For OPTIMAL BATTERY CHARGING FOR DAMAGE MITIGATION

Certificate of Mailing Via Express Mail

I hereby certify that this correspondence was deposited with the United States Postal Service as Express Mail - Label No. EF726146846US - "Express Mail Post Office to Addressee" service in an envelope addressed to BOX PROVISIONAL APPLICATION, Assistant Commissioner of Patents and Trademarks, Washington, D.C. 20231 on this 12 day of June, 2002.

Debbie Tingler, Sec'y to Andrew B. Morton

ASSERTION OF SMALL ENTITY STATUS

Assistant Commissioner for Patents

Washington, D.C. 20231

Sir:

The undersigned attorney, being a representative of The University of Akron, the Assignee of the present invention, hereby asserts that the Assignee is a university of higher education as defined in 37 CFR 1.9 (e)] for purposes of paying reduced fees under section 41 (a) and (b) of Title 35, United States Code, to the Patent and Trademark Office with regard to the above invention described in the specification filed herewith, and therefore entitled to small entity status. Accordingly, when appropriate, small entity fees will be paid during prosecution of this application.

If there are any questions regarding this assertion, a telephone call to the undersigned attorney is requested.

Respectfully submitted,

Ray L. Weber, Reg. No. 26,519
Andrew B. Morton, Reg. No. 37,400
Renner, Kenner, Greive, Bobak,
Taylor & Weber
First National Tower, Fourth Floor
Akron, Ohio 44308-1456
Telephone: (330) 376-1242

Attorney Docket No: UA.439P